Forces on vertical breakwaters:

Effects of oblique or short-crested waves

N W H Allsop
M Calabrese

Report SR 465
March 1999

HR Wallingford

Address and Registered Office: HR Wallingford Ltd. Howbery Park, Wallingford, OXON OX10 8BA
Tel: +44 (0) 1491 835381 Fax: +44 (0) 1491 832233

Contract

The work reported here was part-funded by the Construction Sponsorship Directorate of the (then) Department of Environment (now Department of Environment, Transport & the Regions) under research contract CI 39/5/96 (cc750), and part by the European Union MAST programme under the MCS-Project, contract MAS2-CT92-0047, and later the PROVERBS project, contract MAS3-CT95-0041. Additional support was given by the Department of Hydraulics of University of Naples Federico II, and by the Department of Civil & Structural Engineering of University of Sheffield. Further funding for visiting researchers at Wallingford was awarded from the TECHWARE programme of COMETT, and the National Council for Research in Italy, CNR, and additional support for extended analysis was provided by the Ministry of Agriculture, Fisheries & Food under Flood Defence Commission FD0201.

The project co-ordinator for the MAST III project PROVERBS under contract MAS3-CT95-0041 was Professor H. Oumeraci of Leichtweiss Institute of University of Braunschweig. The project officer for European Commission Directorate General XII was Mr C. Fragakis.

The DETR nominated officer was P.B. Woodhead and HR Wallingford's nominated officer was N.W.H. Allsop. This report is published by HR Wallingford on behalf of DETR, but any opinions expressed are not necessarily those of the research funders.

Prepared by ..... N W H Allsop .....

(name)

..... Manager, Coastal Structures .....

(Title)

Approved by ..... I V. Smith .....

(name)

..... Director .....

(Title)

Date ..... 29th July 1999 .....

Summary

Forces on vertical breakwaters:

Effects of oblique or short-crested waves

N W H Allsop
M Calabrese

Report SR 465
March 1999

Wave forces on vertical breakwaters, seawalls and related structures may be very severe, particularly where waves break against the wall causing impacts loads. Studies at Wallingford presented by Allsop et al (1996) in report SR 443 demonstrated that wave impact loads under normal wave attack are under-estimated by most design methods. The results of that research did however show how conditions that cause wave impacts, and the wave impact forces, can be predicted for long-crested normal wave attack.

It has been generally expected that the occurrence of wave impacts will be substantially reduced under oblique or short-crested wave attack, and that wave pressures / forces will be consequently reduced. Under oblique or short-crested waves, effective wave forces are also expected to reduce on longer caissons. There has however been little or no evidence to support this expectation.

This report gives the results of research studies conducted in the UK national Coastal Research Facility at Wallingford by researchers from Universities of Naples and Sheffield, and HR Wallingford, measuring wave pressures / forces on simple and composite vertical walls under oblique or short crested wave attack. The results of these experiments have been used to compare with existing prediction methods; to identify the ranges of geometric and wave conditions which lead to wave impacts; and to develop new prediction methods for wave pressures / forces under wave impacts.

These results are intended to be used by engineers analysing the stability of vertical or composite walls in deep water, near the coast or along the shoreline. The prediction methods derived here, and/or the test results themselves, may be used to estimate wave loadings on a wide variety of structures, existing or in design.

The work reported here was part-funded by the Construction Sponsorship Directorate of the (then) Department of Environment (now Department of Environment, Transport & the Regions) under DETR research contract CI 39/5/96 (cc750), and part by the European Union MAST programme under the MCS-Project, contract MAS2-CT92-0047, and later the PROVERBS project, contract MAS3-CT95-0041. Additional support was given by the Department of Hydraulics of University of Naples Federico II, and by the Department of Civil & Structural Engineering of University of Sheffield. Further funding for visiting researchers at Wallingford was awarded from the TECHWARE programme of COMETT, and the National Council for Research in Italy, CNR, and additional support for extended analysis was provided by the Ministry of Agriculture, Fisheries & Food under Flood Defence Commission FD0201.

For any further information on these and related studies, please contact Professor N.W.H. Allsop, Manager Coastal Structures at HR Wallingford.

Notation

a	Empirical coefficient
a_e	Air content, used by Partenscky in estimation of extreme wave impact pressures
B, b	Empirical coefficients
B_b	Crest width of rubble mound berm
B_c	Width of caisson, front to back
B_{eq}	Equivalent width of rubble mound in front of wall, averaged over height of mound
B_{wl}	Structure width at static water level, front to back
B_t	Width of rubble mound at toe level
C_β	Pulsating force reduction factor for obliquity
C_{Fh}	Wave impact force reduction factor
C_r	Coefficient of wave reflection
$C_r(f)$	Reflection coefficient function
D	Particle size or typical diameter
D_n	Nominal particle diameter, defined $(M/\rho_r)^{1/3}$) for rock and $(M/\rho_c)^{1/3}$ for concrete armour
D_{n50}	Nominal particle diamter calculated from the median particle mass M_{50}
d	Water depth over toe mound in front of wall
E_i	Incident wave energy
E_r	Reflected wave energy
F_B	Buoyant up-thrust on a caisson or related element
F_S	Factor of safety
F_h	Horizontal force on caisson or crown wall element
$F_{h1/250}$	Mean of highest 1/250 horizontal wave forces
$F_{h,impact}$	Wave impact force (horizontal)
F_u	Up-lift force on caisson or crown wall element
$F_{u1/250}$	Mean of highest 1/250 up-lift wave forces
f	Wave frequency
f_m	Frequency of peak of wave energy spectrum, = $1/T_p$
g	Gravitational acceleration
H_{max}	Maximum individual wave height in design case, sometimes taken as $1.8H_s$
H_{m0}	Significant wave height from spectral analysis, defined $4.0m_0^{0.5}$
H_{so}	Offshore significant wave height, un-affected by shallow water processes
H_s	Significant wave height, average of highest one-third of wave heights
H_{sb}	Breaking significant wave height
H_{si}	Incident significant wave height, taking account of all shallow water processes
h	Water depth
h_b	Height of berm above sea bed
h_{br}	Water depth at point of breaking
h_c	Height of rubble mound / core beneath caisson / wall
h_f	Exposed height of caisson or crown wall over which wave pressures act
h_s	Water depth at toe of structure

k	Wave number = $2\pi/L$
K_L	Wave impact coefficient used by Partenscky = 5.4 (($1/a_e$) – 1)
L	Wave length, in the direction of propagation
L_c	Length of individual caisson
L_{mo}	Offshore wave length of mean (T_m) period
L_o	Deep water or offshore wave length - $gT^2/2\pi$
L_{po}	Offshore wave length of peak (T_p) period
L_{ps}	Wave length of peak period at structure
M_h	Overturning moment due to horizontal wave force
M_u	Overturning moment due to up-lift force
M_t	Overturning moment due to all wave loads
m_0	Zeroth moment of the wave energy density spectrum
m_2	Second moment of the wave energy density spectrum
m	Sea bed slope or gradient
N_{wo}	Number of waves overtopping expressed as proportion or % of total incident
N_z	Number of zero-crossing waves in a record = T_R/T_m
P	Total horizontal load derived by Goda's method; also encounter probability
P_f	Target probability of failure
$P_{i\%}$	Percentage impacts, with respect to incident waves
p	Wave pressure
p_1, p_2, p_3, p_u	Wave pressures acting at points on wall calculated by Goda's method
p_{av}	Average wave pressure, usually over (vertical) face of wall
p_{dyn}	Dynamic or impact pressure, used by Partenscky
p_i	Wave impact pressure
q	Mean overtopping discharge, per unit length of structure
R_c	Crest freeboard, height of crest above static water level
R_u	Run-up level, relative to static water level
$R_{u2\%}$	Run-up level exceeded by 2% of run-up crests
r	Roughness or run-up reduction coefficient, usually relative to smooth slopes
S_F	Shear force at caisson / rubble boundary
$S(f)$	Spectral density
s_m	Steepness of mean wave period = $2\pi H/gT_m^2$
s_p	Steepness of peak wave period = $2\pi H/gT_p^2$
T_m	Mean wave period
T_{Pf}	Return period = $(1 - (1 - P_f)^{1/T})^{-1}$
T_p	Wave period of spectral peak, inverse of peak frequency
T_R	Length of wave record, duration of sea state
u, v, w	Components of velocity along x, y, z axes
v_c	Wave velocity, used by Blackmore & Hewson
x, y, z	Orthogonal axes, distance along each axis
z	Level in water, usually above seabed
α	Structure front slope angle to horizontal
α_1, α_2	Coefficients in Goda's method to predict wave forces on caissons

β	Angle of wave attack relative to breakwater alignment
η_0	Extreme run-up level
ρ_w	Mass density of sea water
ρ_r, ρ_c, ρ_a	Mass density of rock, concrete, armour units
λ	Aeration factor used by Blackmore & Hewson
μ (mu)	Coefficient of friction, particularly between concrete elements and rock
ξ (xi)	Iribarren number or surf similarity parameter, = $\tan\alpha/s^{1/2}$
ξ_m, ξ_p	Iribarren number calculated in terms of s_m or s_p
θ, θ_0	Wave direction, and central wave direction

Contents

Tables

Figures

Appendices

1. INTRODUCTION

Harbour breakwaters may be of two general forms: impermeable (to wave action) with steep or vertical faces; or permeable with sloping faces. Much research effort has been devoted to the stability and hydraulic performance of rubble mound structures, see for instance the CIRIA / CUR Rock Manual edited by Simm (1991), but less research has been devoted in UK and Europe to the stability of vertical walls and related structures with steep faces, impermeable to wave action. This report is one of two describing research studies on wave loadings on vertical and composite walls, and presenting improved prediction methods and data on wave forces for such structures formed from blockwork, large concrete caissons, or other materials. These studies follow earlier work at Wallingford on the hydraulic performance of simple vertical walls, and variations that incorporate perforated screens and/or voided chambers, see Besley et al (1998), Allsop (1995), McBride & Watson (1995) and McBride et al (1995).

The companion report on wave forces (Allsop NWH, Vicinanza D, & McKenna JE "Wave forces on vertical and composite breakwaters" Strategic Research Report SR 443, HR Wallingford, March 1996, Wallingford) describes the main types of vertical and composite breakwaters, and summarises present and extended prediction methods for horizontal and up-lift wave pressures. It describes new research studies, and analysis and discussion on new or revised prediction methods. The tests and analysis described in SR 443 were however confined to two-dimensional (2-d) normal wave attack. This report therefore describes further three-dimensional (3-d) tests conducted in the UK Coastal Research Facility (CRF) to identify the extent to which oblique or short-crested waves change wave loads on long structures.

The work reported here was part-funded by the Construction Sponsorship Directorate of the then Department of Environment (now Department of Environment, Transport & the Regions, DETR) under research contract CI 39/5/96 (cc750) and part by the European Union MAST programme under contract MAS3-CT95-0041, the PROVERBS project. Additional support was given by the "Programme for International Exchange of Researchers" of University of Naples Federico II, with further funding for visiting researchers at Wallingford from the TECHWARE programme of COMETT, and the National Council for Research in Italy. Additional research support was given by the University of Sheffield.

1.1 The problem

European and UK consultants and contractors are involved in analysis, design, rehabilitation, and construction of harbour and coastal structures world-wide, and particularly in the design of large breakwaters. UK / European design methods / codes are used internationally, so it is particularly important that such methods are well-based and reliable.

Breakwaters and related structures are built primarily to give protection against wave attack to ship moorings, manoeuvring areas, port facilities, and adjoining areas of land. Design methods for most types of structures are generally well established, but important aspects of those design methods are now seen to be uncertain or of limited application for some configurations. Wave pressures / forces are the source of the main design loads acting on most harbour breakwaters and related marine or shoreline structures. Recent practical experience, and research results analysed under UK and EU's MAST research programmes, have shown that design methods for such loads are uncertain and insufficient, and may therefore be unsafe for some structures. Research studies have therefore been conducted to provide new design data and prediction methods on wave loadings on these structures.

If wave attack is normal to the wall, and acts uniformly on a long length of structure, the total wave force can be very large. That force may however be predicted by assuming simple normal wave attack and using methods described in SR 443. Under conditions of waves and structure geometry discussed in SR 443, wave momentum is converted to short and intense wave impact pressures. The total wave force under these impacts are substantially greater than those forces predicted by generally-accepted design methods, but wave impact forces only persist for very short durations. Most of the studies of wave impact forces, have however been confined to narrow (2-dimensional) wave flumes with normal wave attack.

It is however often argued that severe storm waves are usually short-crested, other than in relatively shallow water, and that therefore the largest wave loads will not apply uniformly along any significant length of the structure at one time. It may also be assumed that wave impact forces are essentially local, and that their effect reduces over any significant length of the breakwater. These arguments may all be used to justify reductions in the wave forces, and the possibility of quantifying these reductions is important

for practical design projects. There is however very little reliable information available to support such reductions.

1.2 Terms of reference for the study

The primary objective of the work commissioned by DETR under contract CI 39/5/96 (cc750) was to provide additional design data for vertical faced breakwaters and related structures on wave loads under oblique or short-crested wave attack. The programme of work identified at the start of the studies was summarised:

a) Review most recent data from MAST MCS project on critical wave conditions, obliquities, and wave spreading.
b) Design model tests for caisson sections in the CRF, construct caisson sections; instrument caisson test section for pressures / forces.
c) Complete parametric wave basin tests for selected structure configurations for oblique, long- and short-crested wave conditions. Measure spatial variations of local pressure gradients.
d) Complete analysis to identify the influence of oblique wave attack and/or short-crested waves on wave forces. Analyse spatial variations of local pressures / gradients.
e) Present study results in empirical formulae / graphs. Derive general design rules.

The studies on wave loadings discussed here were expanded to include contributions from researchers from University of Naples developed in collaboration with HR and University of Sheffield.

1.3 Outline of the studies

The use of the UK Coastal Research Facility imposed a number of constraints on the project. Of these the most important were that it was not possible to modify the model sea bed, particularly the 1:20 approach beach; and that the period available in the CRF programme was limited to 9 October to 10 November 1995. In contrast, it may be noted that the 2-d flume tests reported in SR 443 took at least 3 months to complete. Detailed model design, preparation of test sections and instrumentation for these 3-d tests had therefore to be completed by end September 1995, and testing was completed by mid November.

As will be shown later, this restricted test period did not cause significant limitation to the output of the study. The testing built upon the substantial dataset measured in the previous 2-d study, and took full advantage of careful planning of the structure geometries and of wave conditions to be tested. The very restricted time available for testing did however force all analysis of measurements to be conducted afterwards, substantially increasing the difficulty of analysis.

Analysis of the considerable volume of data was more complex than in the 2-d studies, and initial data processing was completed during January 1996. Initial analysis of the main results was completed during February - March and August - September 1996, but further analysis and interpretation was completed in 1997 and 1998.

1.4 Outline of this report

As a companion report to SR 443, this report follows a similar sequence. The main types of vertical walls in use in harbours or along coastlines were however described previously in SR 443, so relatively little detail is given here. Particular design methods to predict the effects of oblique or short-crested wave attack are described here in Chapter 2, thus supplementing the detailed descriptions given previously in Chapter 3 of SR 443.

The design of the CRF experiments in this study, the structure configurations tested, and the test equipment and procedures are described in Chapter 3.

Analysis of the wave pressure / force measurements are described in Chapter 4, which discusses detailed forces for normal, oblique or short-crested wave attack for simple vertical and composite walls.

Application of the wave force results, and the prediction methods derived from them are discussed in Chapter 5. Overall conclusions, and recommendations for design / analysis practice, and for future research, are addressed in Chapter 6.

2. PREVIOUS RESEARCH AND CURRENT DESIGN METHODS

Wave forces on vertical breakwaters or seawalls or related structures may be very severe, particularly where waves break directly against the wall causing impacts loads. Results of new research studies on wave loads on vertical and composite structures under normal wave attack have been presented by Allsop et al (1996), but those studies gave no guidance on the influence of wave obliquity, on the influence of short crested waves, nor on any variability in wave loading on longer caissons. This report has not repeated the review of methods described in SR 443, but simply identifies reports / papers which are concerned with the effects of oblique or short-crested waves. It is however useful to summarise here the main prediction methods reviewed in the earlier study

Under oblique or short-crested wave attack, it is generally expected that the occurrence of impacts will be reduced, and that wave loads will consequently be reduced. Furthermore, the effective wave load on large caisson elements is expected to reduce under oblique waves or short-crested attack as the load is spread over a greater length. These suggestions are the reviewed later against previous studies and/or design recommendations.

2.1 Summary of design methods

It is often convenient to treat wave pressures or forces in two categories, see Figure 2.1:

Quasi-static, or pulsating;
Dynamic, impulsive or impact

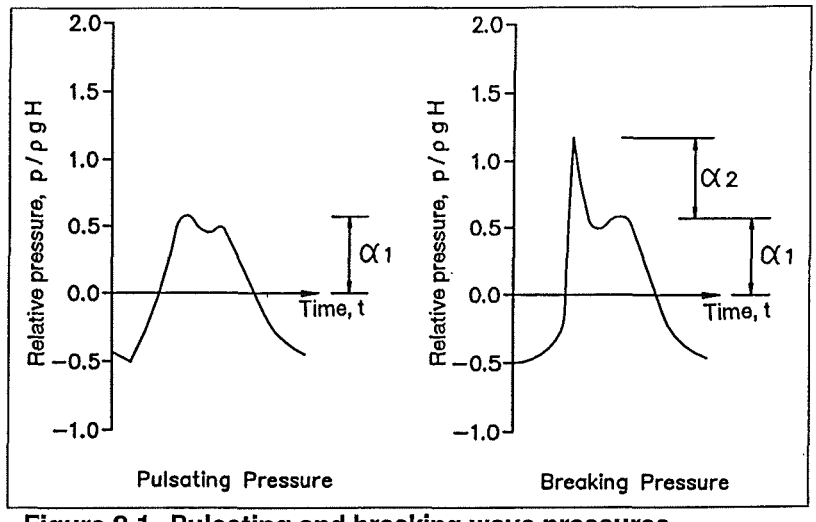

Figure 2.1 Pulsating and breaking wave pressures

Quasi-static or pulsating wave pressures change slowly. Quasi-static forces arise as the wave crest impinges directly against the structure applying a hydro-static pressure difference, and obstruction of wave momentum causes the wave surface to rise up the wall, increasing the pressure on the wall. Pulsating wave forces are approximately proportional to the wave height, and can be estimated using relatively simple methods.

Dynamic or impact pressures are caused by the special conditions that arise where a wave breaks over a beach, steep seabed or mound onto the structure. Impact pressures are substantially greater than pulsating pressures, but of shorter duration. Detailed processes of wave breaking are not well understood, and impact pressures are extremely difficult to calculate reliably.

The main methods used in design manuals to estimate wave forces on upright walls, breakwaters or seawalls, have been derived by:

Hiroi and Ito for simple walls
Sainflou for simple walls
Goda for caisson breakwaters
Goda / Takahashi for composite breakwaters
Minikin for breaking waves composite walls
Blackmore & Hewson for broken waves on seawalls
Jensen / Bradbury & Allsop for crown walls

The most widely used prediction method for wave forces on vertical walls was developed by Goda (1974, 1985). This method is described in 2.2 below, and is applied in BS6349 Pt 1, BSI (1984). Before considering Goda's method in detail, it is however useful to review briefly previous methods, particularly those by Ito, Hiroi and Sainflou, see Ito (1971), and by Minikin (1963).

Hiroi's formula gives a uniform wave pressure on the front face up to 1.25H above still water level:

$$p_{av} = 1.5\rho_w g H \qquad (2.1)$$

where p_{av} = the average wave pressure, and H is a design wave height, probably H_{max}, but may be set to $H = H_{1/3}$, see discussion below.

Sainflou's method derives a pressure distribution with maximum, p_1 at static water level, tapering off to zero at a clapotis height above s.w.l. of $H+\delta_0$, and reducing linearly with depth from p_1 to p_2 at the rubble base:

$$p_1 = (p_2 + \rho_w g h)(H + \delta_0) / (h + H + \delta_0) \qquad (2.2a)$$
$$p_2 = \rho_w g H / (\cosh(2\pi h/L)) \qquad (2.2b)$$
$$\delta_0 = (\pi H^2/L) \coth(2\pi h/L)) \qquad (2.2c)$$

Ito discusses the use of Hiroi's formula where the water depth over the mound, d, is less than $2H_{1/3}$, and Sainflou's methods when $d>2H_{1/3}$. It is interesting to note that Sainflou's method generally gives pressures of about $0.8\text{-}1.0\rho_w g H$, rather smaller than Hiroi's.

In Japan, there was some uncertainty whether Hiroi's method gave safe results when using $H=H_{1/3}$. There were additional concerns over the effects of waves breaking over the mound. A simple method by Ito, discussed by Goda (1985) gave a rectangular distribution of horizontal pressures acting on the front face of the caisson, calculated in terms of H_{max}. The value of H_{max} is $2H_s$, or H_{bmax} if waves are depth-limited. The pressure, p_{av}, is then determined for 2 different regions of relative water depth, H/h_s. Ito assumed a triangular up-lift pressure distribution, but uniform pressures on the vertical face:

$$p_{av} = 0.7\rho_w g H_{max} \quad \text{for } H<d \qquad (2.3a)$$
$$p_{av} = \rho_w g H_{max}(0.15 + 0.55H/d) \quad \text{for } H>d \qquad (2.3b)$$

Minikin's method was developed in the early 1950s' to estimate local wave impact pressures caused by waves breaking directly onto a vertical breakwater or seawall. Minikin used Bagnold's piston model and calibrated a version of this model with pressure measurements on a sea wall at Dieppe by Rouville to give maximum peak pressures for typical wave impact events. Unfortunately, Minikin's formula was re-written with $\pi\rho_w g$ replaced by 2.9 in units of tons (force) per square foot. This was later compounded by other authors, including the Shore Protection Manual, which re-wrote Minikin's formula with πg replaced by 101 with added confusion over the use of tons or tons force.

After Minikin, some attention has been devoted to quantifying wave impact pressures more reliably. At small scale, very large (relative) pressures may be measured if small fast-responding transducers are sampled very rapidly. At large scale, Partenscky used results from the large wave channel at Hannover / Braunschweig (GWK) to suggest that impact pressures of very short durations (0.01 to 0.03s) may be calculated from:

$$p_{dyn} = K_L \rho_w g H_b \qquad (2.5a)$$

where H_b is a breaking wave height, and the coefficient K_L is given in terms of the air content a_e of the breaking wave:

$$K_L = 5.4 ((1/a_e) - 1) \qquad (2.5b)$$

Blackmore & Hewson (1984) conducted field measurements at four sea walls in the UK, from which they developed a model based on momentum exchange. Impact pressures p_i depend on the shallow water wave velocity, v_c; the wave period, T; and an aeration factor, λ, which depends on foreshore roughness:

$$p_i = \lambda \rho_w T v_c^2 \qquad (2.6a)$$

A value of $\lambda = 0.3$ is recommended for a rough and rocky seabed, and $\lambda = 0.5$ for a regular seabed. Breaking wave heights are indirectly considered by using shallow water wave velocities calculated from the breaking water depth, h_{br}, and breaking wave height, H_b:

$$v_c = [\, g\,(h_{br} + H_b)]^{0.5} \qquad (2.6b)$$

2.2 Goda's method

Of the design methods reviewed in SR 443 by Allsop et al (1996), only the method by Goda (1985) gives any estimate of the effect of wave obliquity. This method is also adopted in British Standard 6349, BSI (1984) and the CIRIA / CUR rock manual edited by Simm (1991). Most comparisons in this and the previous report are therefore made with this method.

The general philosophy behind Goda's method is deterministic, with the emphasis on the single extreme wave (or force event) that could cause sliding. The exceedance level chosen for this prediction method was the average of the top 1/250 events, and it is this exceedance level that has been taken as de facto standard for wave force calculations for these types of structures. Horizontal and uplift forces calculated by this approach have therefore been termed $F_{h1/250}$ and $F_{u1/250}$.

If (pulsating only) wave forces may be assumed to follow a Rayleigh probability distribution, forces at other exceedance levels might be estimated from the following ratios of $F_{i\%}/F_{1/250}$:

Exceedance level	$F_{i\%}/F_{1/250}$
50%	0.33
90%	0.59
98%	0.77
99%	0.84
99.5%	0.90
99.8%	0.97
99.9%	1.03

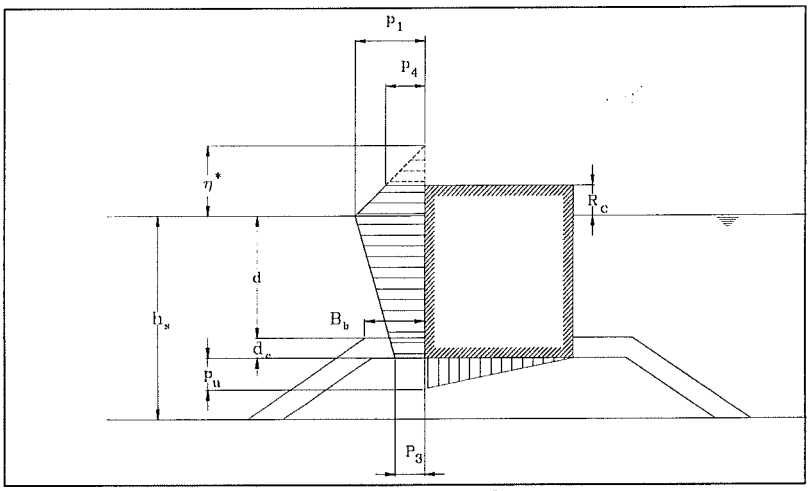

Figure 2.2 Goda's pressure distributions

Goda's method represents the wave pressure response by considering two components, the breaking wave and the deflected wave (slowly - varying pressure) represented in the method by coefficients α_1, α_2, and α_3.

In Goda's approach, α_1 represents the slowly varying pressure component and α_2 represents a contribution due to the breaking pressure component. The coefficient α_1 is influenced by the relative depth to wavelength and α_2 is influenced by the relative level of the mound. The last of the coefficients, α_3 accounts for the relative crest level of the caisson and the relative water depth over the toe mound.

Wave pressures on the front face are assumed to be distributed trapezoidally, reducing from p_1 at the static water level (s.w.l.) to p_2 at the caisson base, Figure 2.2. At points above s.w.l., pressures reduces to zero at the notional run-up point given by a height η^*. Underneath the caisson, up-lift pressures at the seaward edge are determined by a separate expression, and may be less than pressures calculated for the toe of the seaward face. In Goda's method, up-lift pressures are distributed triangularly from the seaward edge to zero at the rear heel. The main response parameters are determined from:

$$\eta^* = 0.75(1+\cos\beta)H_{max} \qquad (2.7a)$$

$$p_1 = 0.5(1+\cos\beta)(\alpha_1+\alpha_2\cos^2\beta)\rho_w g H_{max} \qquad (2.7b)$$

$$p_2 = p_1 / (\cosh(2\pi h/L)) \qquad (2.7c)$$

$$p_3 = \alpha_3 p_1 \qquad (2.7d)$$

$$p_u = 0.5(1+\cos\beta)(\alpha_1\alpha_3)\rho_w g H_{max} \qquad (2.7e)$$

The coefficients α_1, α_2, and α_3 are determined from:

$$\alpha_1 = 0.6 + 0.5 \left[(4\pi h/L)/\sinh(4\pi h/L) \right]^2 \quad (2.8a)$$

$$\alpha_2 = \min\{ ((h_b-d)/3h_b)(H_{max}/d)^2 , 2d/H_{max} \} \quad (2.8b)$$

$$\alpha_3 = 1 - (h'/h) \left[1 - 1/\cosh(2\pi h/L) \right] \quad (2.8c)$$

Where η^* is the maximum elevation above s.w.l. to which pressure could be exerted (taken by Goda as $\eta^* = 1.5H_{max}$ for normal wave incidence) β is the angle of wave obliquity in plan, see Figure 2.3. The design wave height, H_{max} is taken as $1.8H_s$ for all positions seaward of the surf zone. In conditions of broken waves, H_{max} should be taken as H_{maxb}. The water depth h is taken at the toe of the mound, so $h = h_s$, or as $h = d$ over the mound at the front face of the caisson, but h_{br} is taken $5H_s$ seaward of the structure.

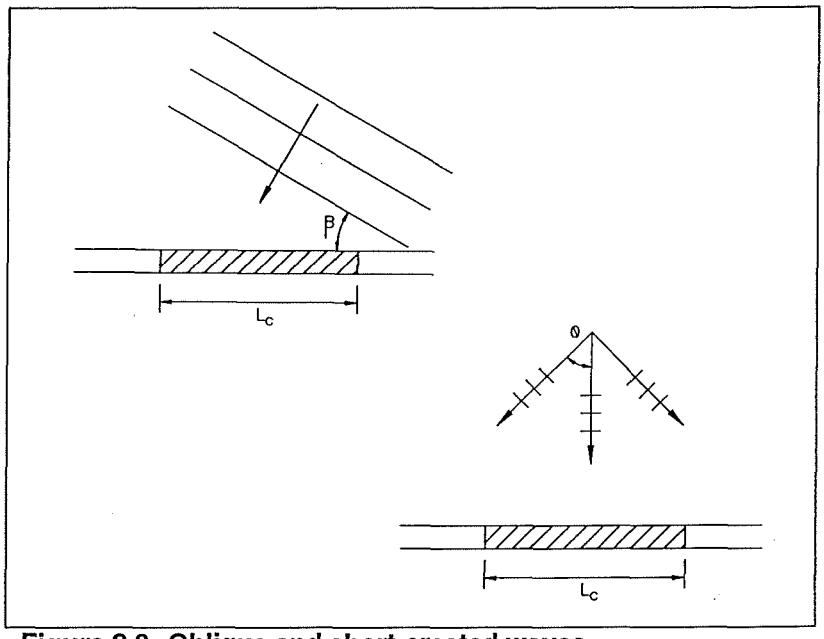

Figure 2.3 Oblique and short-crested waves

The effects of wave obliquity β to the caisson face (see Figure 2.3) appear in expressions η^*, and for p_1, p_u in which a general reduction factor of $0.5(1+\cos\beta)$ is used. This gives a very simple way to estimate the effect of wave obliquity on the reduction of effective momentum for pulsating waves. The coefficient α_2 is modified by the reduction factor $\cos^2\beta$ to cover the influence of obliquity on impulsive pressures. On this point Goda (1985) argues that the angle of incidence to the breakwater is important in reducing breaking wave pressures. Impulsive pressures decrease rapidly at larger obliquities due to the decrease in the normal component of the momentum of the wave, proportional to $\cos^2\beta$. Impulsive pressures will further reduce as the effective duration of the impact peak pressure on the caisson increases as obliquity increases.

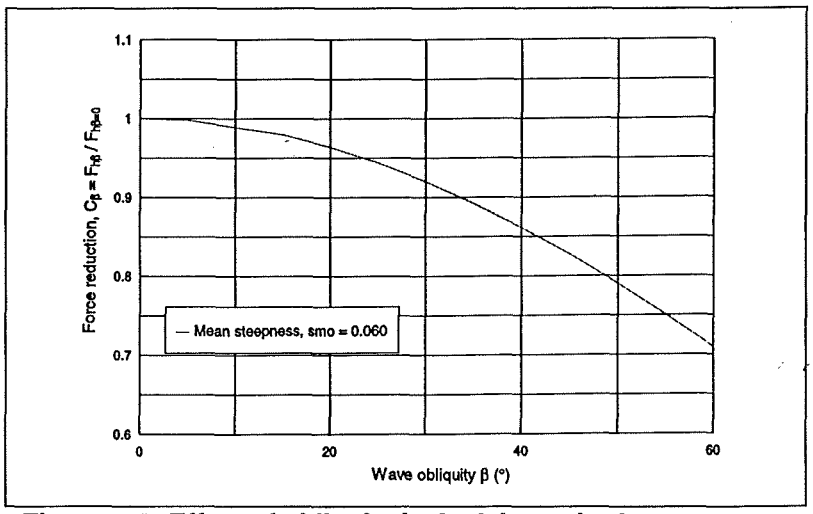

Figure 2.4 Effect of obliquity in Goda's method

The effects of obliquity β on the force relative to normal wave attack using Goda's method are illustrated in Figure 2.4 for two wave steepnesses and a simple vertical wall as used in this study. Wave forces reduce steadily with obliquity. At β=45°, (the greatest angle used in these tests) wave forces predicted by Goda's method reduce to 80-85% of those due to normal waves.

Wave steepness has a small effect on the force decay, becoming greater with obliquity. The maximum variation in force decay (at β=60°) between waves of s_{mo} = 0.026 and waves of s_{mo} = 0.059 is, however, only 1%. This suggests that the influence of wave steepness on force decay with obliquity may therefore be ignored in all practical instances.

Indeed, the effect of small values of obliquity are also relatively mild. In Japanese practice, it is argued that it is difficult to estimate angles of obliquity with precision, so it is recommended that the threshold angle should be β=15°. For incident angles of $\beta \leq 15°$, wave attack is assumed to be normal (as if β=0°), and no reduction is applied. For obliquities β>15°, Japanese practice as described by Goda (1995) recommends that the true angle of obliquity be reduced by 15°, taking account of the relatively wide directional sectors in which wave directions may be determined from wind information. In practice in Japan, Goda's full prediction method discussed above is therefore only used for values of β-15°. This adjustment of incident wave angle is intended to cover both uncertainties in estimation of wave direction and directional spreading.

Goda's method was reviewed in Tanimoto (1976) to assess any additional allowance for increased impulsive pressures. This analysis suggested that impulsive pressures are unlikely when $\beta \geq 20°$.

2.3 Battjes' method

Under normal and long-crested wave attack, the same wave forces are assumed to act at all points along the wall, thus not changing over the length of any wall or caisson element. When waves approach a vertical (or composite) wall at an oblique angle however, the effective wave forces act over a reduced length of wall at any one time. As the length of any individual caisson, L_c, increases, the effective wave load is averaged over a greater length, and will thus reduce relative to the load under simple normal attack.

Battjes (1982) developed a theoretical model to calculate the reduction in effective load as a function of caisson length relative to incident wavelength and wave obliquity. The reduction in effective load C_β is:

$$C_\beta = [\sin(\pi \sin\beta (L_c/L)) / (\pi \sin\beta (L_c/L))] \qquad (2.9)$$

where β is the wave obliquity and L_c/L is the relative caisson length to wavelength.

Battjes' theoretical model focussed on a single wave period T, or wave length L. For random seas, it is probable that the most appropriate wave period to use in the estimation of a force reduction factor is the peak wave period, T_p. As Battjes' method is based on linear wave theory, it is appropriate to use the simple deep water wave length, based on the peak period, L_{op}.

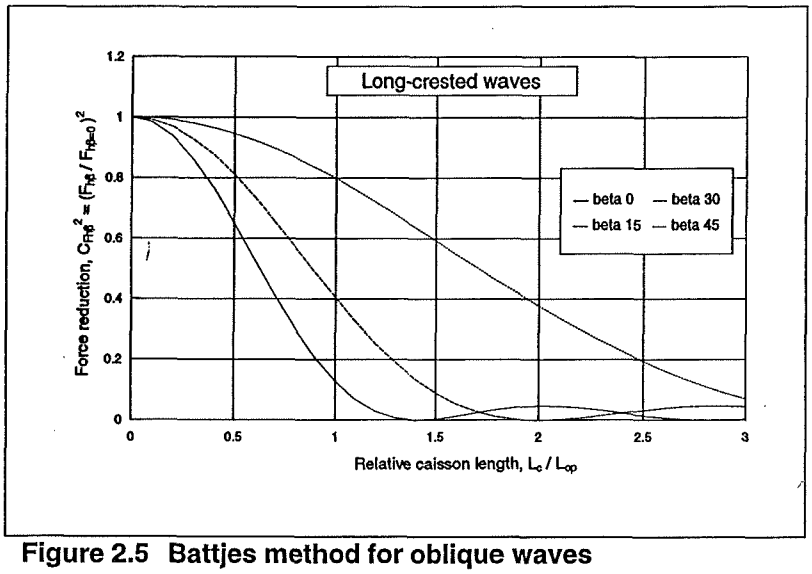

Figure 2.5 Battjes method for oblique waves

The form of this relationship is presented for values of β=0, 15, 30, and 45° in Figure 2.5. Battjes' analysis is based on the use of linear wave theory, and therefore assumes non-breaking waves. This method also predicts that the wave obliquity has no effect on an infinitesimally short segment of the wall, thus C_β = 1 at a relative caisson length of zero, L_c/L=0. It may be noted that Goda's method does give reduced pressures under oblique attack irrespective of caisson length, but that method was developed from model tests and field data analysis in which the caissons always had finite lengths, typically 15-30m and Battjes' method generally gives greater reductions for obliquity (lower values of C_β) than Goda's method for increasing caisson lengths relative to wave length.

2.4 Short-crested wave attack

In many situations, waves at a breakwater in deep water will be short-crested, with a distribution of energy over a range of angles θ around the mean wave direction, θ_0. Even if the mean wave direction is itself

normal to the structure, much of the incident energy over the other directions will be oblique to the wall. Furthermore, any wave crest will be relatively short, so will act over only a part of the length of a caisson. It might, therefore, be expected that short-crested waves will give rise to smaller loads than long-crested waves.

Battjes (1982) developed a theoretical model to estimate the load reduction over relative caisson lengths L_c/L for short-crested waves. Wave spreading of a short-crested sea is expressed by a directional distribution function, D, where:

$$D = D_n(\theta, \theta_0) = A(n) \cos^n(\theta - \theta_0) \qquad |\theta - \theta_0| \leq \pi/2 \qquad (2.10a)$$

$$D = 0 \qquad |\theta - \theta_0| > \pi/2 \qquad (2.10b)$$

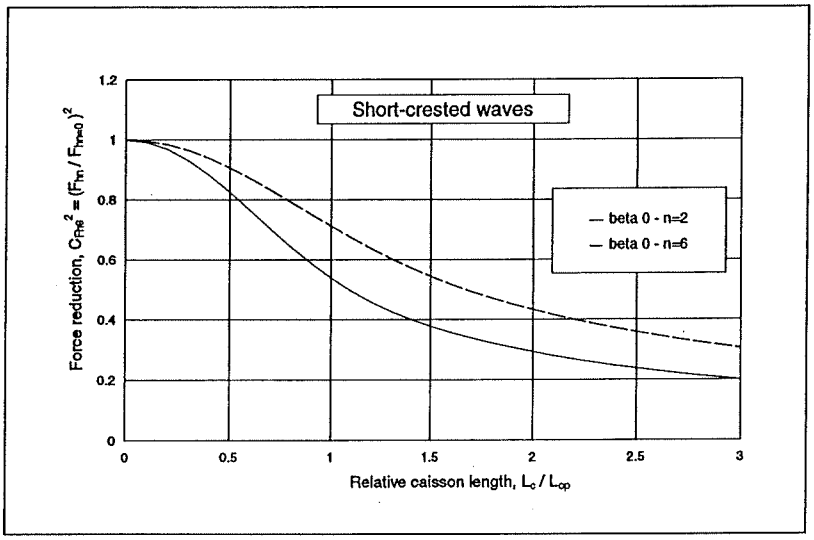

Figure 2.6 Battjes method for short-crested waves

Using this definition of directional spreading, a value of n=2 (i.e. $\cos^2(\theta - \theta_0)$ corresponds to wide spreading, and is generally regarded as appropriate for open ocean conditions. A value of n = 6 (i.e. $\cos^6(\theta - \theta_0)$ corresponds to moderate spreading; and n = 30 (i.e. $\cos^{30}(\theta - \theta_0)$ corresponds to very narrow spreading, close to long-crested. The directional spreading index, n, is assumed to be constant with wave frequency. The value of A(n), a normalisation factor, given by:

$$A(n) = \tfrac{1}{2} \qquad (2.11a)$$

where n = 1

$$A(2) = 2/\pi \qquad (2.11b)$$

where n = 2

$$A(n) = [n/(n-1)]\, A(n-2) \qquad 2.11c)$$

where n = 3, 4, 5,

such that:
$\int_{-\pi}^{+\pi} D(\theta; \omega)\, d\theta = 1$
for all ω where ω is the angular frequency.

The effect of the short-crestedness on the load is expressed by:

$$C_\theta = \int_{-\pi}^{+\pi} C\beta^2\, D(\theta; \omega)\, d\theta \qquad (2.12a)$$

This reduction factor is applied to the load per unit length, given values of the directional spreading index and mean wave direction. The reduction of C_θ with increasing L_c/L_p is shown in Figure 2.6. The reduction of wave forces is more marked with increasing wave spreading, as shown by the curve for n=2 compared to n=6. This method predicts that the wave spreading has no effect on an infinitely short segment of the wall, thus $C_\beta = 1$ at a relative caisson length of zero, $L_c/L=0$.

The maximum force on a structural element of length L_c is given by:

$$P(L_c) = C_\theta^{0.5}\, P(0) \qquad (2.12b)$$

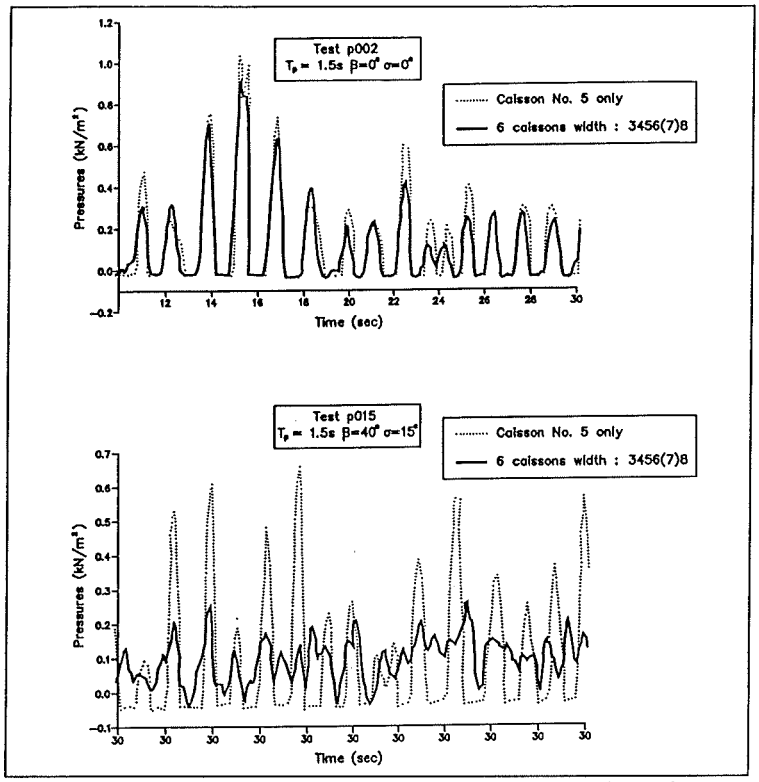

Figure 2.7 Example results from Franco et al (1995)

2.5 Recent experimental studies

Experimental studies by Franco et al (1995) investigated some of these issues in hydraulic model tests in a large wave basin at Delft Hydraulics, under the Large Installations Programme (LIP) of the EC. These tests measured wave forces, and pressures for a number of adaptations of a simple caisson on a small mound. The structure was made up of thirteen caissons , each 0.9m long, making the overall length 11.7m. The water depth in front of the mound was 0.61m, and the height of the mound was 0.133m. The height from the top of the caisson to the seabed varied between 0.700m and 0.838m depending on the height of the caisson parapet. Wave forces were measured at one point along the caisson with a force plate, and pressures were measured with transducers at other locations along the series of caissons.

A single water level, and a single wave height were used in the LIP tests, equivalent to H_{si}/h_s=0.23 at wave steepnesses of s_{op} = 0.02 and 0.04. The tests used 3 degrees of wave spreading, with normal attack and with 6 angles of obliquity. An example of the load decay with increasing caisson length is shown in Figure 2.7 which contrasts pressure signals at the water level for a single caisson, with pressures averaged over 6 caissons. It is particularly interesting to note that these results show reductions in the load with increasing caisson length, even under long-crested normal waves. This suggests that there was always some degree of short-crestedness in Franco's tests, perhaps due to variability in the waves reflected back towards the test sections. Under (intentionally) oblique short-crested waves, the reduction is again more severe, that is the value of C_θ is smaller.

Franco found that Goda's method gave reasonable estimates of the (pulsating) horizontal force under three-dimensional waves, but that there was considerable scatter in the results. For the long-crested waves the reduction of horizontal load with wave obliquity was fairly well described by Goda. Under short-crested waves, however, the experimental results showed no reduction in the wave forces with wave obliquity. This effect is not described by Goda. Franco suggests a reduction factor for use under "three dimensional seas" - assumed to mean "short crested waves" - of 10% which remains constant for all wave obliquities.

The reduction of load with increasing caisson length under long-crested waves for large values of L/L_p was found to be greater than Battjes predictions based on linear wave theory. Under short-crested waves, however, the agreement with Battjes was fairly good. Comparison of Franco's results with results from these tests are discussed in Chapter 5.

2.6 Conclusions from previous work

Previous experimental work by Goda (1985) and by Franco et al (1996), taken together with the theoretical analysis by Battjes (1982), suggests that the effects of wave obliquity, short-crestedness, and caisson length on pulsating waves are relatively easy to predict. Design methods have been described for the influence of wave obliquity and/or short-crested waves on pulsating wave loads, and are generally supported by the short series of experiments reported by Franco et al (1996).

There is however no information on the effects of obliquity and/or short-crestedness on wave impact loads. As this type of wave load is now seen to be more likely than hitherto assumed, and consequences of wave impact loads are now seen to be of considerable potential importance, it is important to identify the

potential for occurrence of wave impact loads under more practical conditions than those used in simple 2-d wave flume tests.

Another aspect of wave impact loads that has been touched upon, but not answered, is the spatial extent of wave impact loads, even under (nominally) normal and long-crested wave attack. It is clear that there is inevitably some degree of inhomogeneity in any wave attack on a realistic structure, and this may be sufficient to provide a spatial limit to wave impact loads. There are however no data or guidance on the likely spatial extent of such loads.

3. DESIGN OF RESEARCH STUDIES

3.1 Overall plan of studies

The main variables that influence wave forces on vertical and composite walls include the following geometric and wave parameters:

a) significant offshore or inshore wave heights, H_{so} and H_{si};
b) water depth in front of the structure, h_s; and crest freeboard, R_c;
c) wave steepness, s_m; and hence wave length at structure toe, L_s;
d) water depth over mound in front of wall, d; and hence berm height, h_b;
e) berm width, B_b;
f) front slope of mound, α;
g) depth of embedment of caisson into mound, h_b-h_c;
h) sea bed approach slope, m
l) angle of wave attack, β;
j) spreading of wave attack, $\cos^n$.

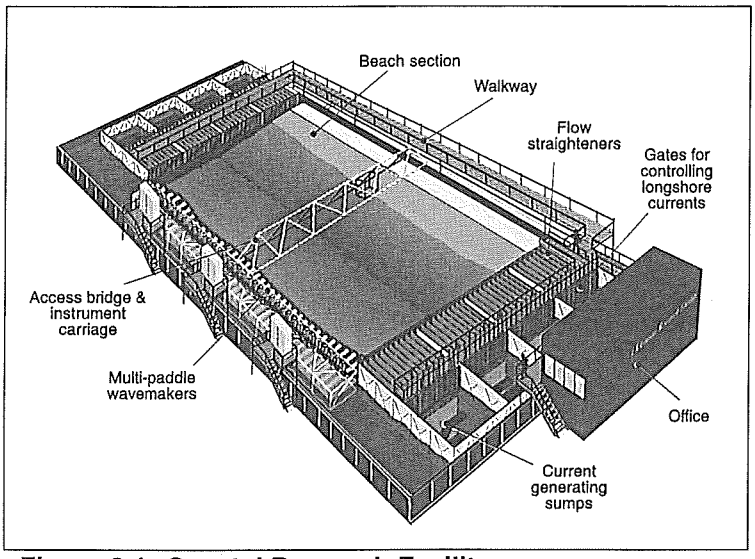

Figure 3.1 Coastal Research Facility

A test programme could have been devised to study each of these parameters systematically, but this would have required many hundreds of tests, occupying the basin for many months. Given the strict limitations on the test programme in the CRF (Figure 3.1), a drastic reduction of the range of variables was devised. Many of the parameters identified in items a) to g) had been studied previously in the 2-dimensional (2-d) studies discussed by Allsop et al (1996). It was therefore not felt that it was necessary to investigate again many of these parameters.

Storm waves around the coastlines of Europe are generally associated with wave steepnesses of about s_{mo}=0.04 to 0.06. It is known that some wave functions are strongly geared to wave steepness, so tests were run for both these steepnesses, as well as for a lower steepness, s_{mo}=0.02. This compares directly with the wave steepnesses employed earlier in the 2-dimensional tests.

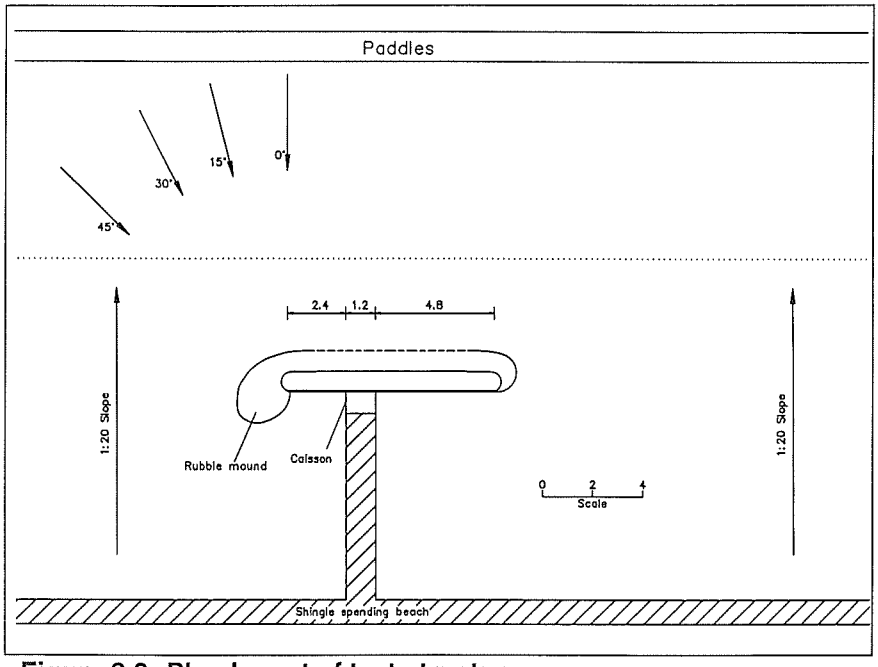

Figure 3.2 Plan layout of test structure

The model was designed to be tested at 2 water levels (0.77m and 0.68m above the basin floor, model dimensions). Both water levels were used, but not for all combinations of wave heights and wave direction. The water levels selected corresponded to levels used in the earlier studies and were believed to provide maximum forces on the caisson structure.

The wave heights used in the basin were limited in absolute magnitude by the capacity of the wave generator, but were varied between H_{si} = 0.1 and 0.25m. For the simple vertical wall, values of the relative wave height H_{si}/h_s varied between H_{si}/h_s = 0.12 to 0.53. So for a prototype breakwater in a depth of 20m of water, this gives a notional model scale of approximately 1:40, and a range of wave conditions equivalent to H_{si} = 4 – 10m. This range covers most wave exposures around the Mediterranean, much of the North Sea, and many other coastlines around the world.

For the simple vertical wall, the parameters varied were limited to the wave conditions, local water depth and wave attack angle. The crest level of the caisson was not changed, although its freeboard varied as a consequence of the two different water depths. The influence of test duration upon the upper limits of the wave force induced on the caisson was studied, the majority of tests were run for a duration of 500 waves, but a small number were repeated with a duration of 2000 waves. A small number of tests were conducted to determine whether forces on the caisson were different depending from which side of the basin the waves approached.

For the composite structure, the wave attack angle was varied together with changes to the relative height / depth of rock armoured berm in front of the caisson. Three different relative heights were studied. A single berm width of 0.25m together with a front armour slope of 1:2 were maintained for this study.

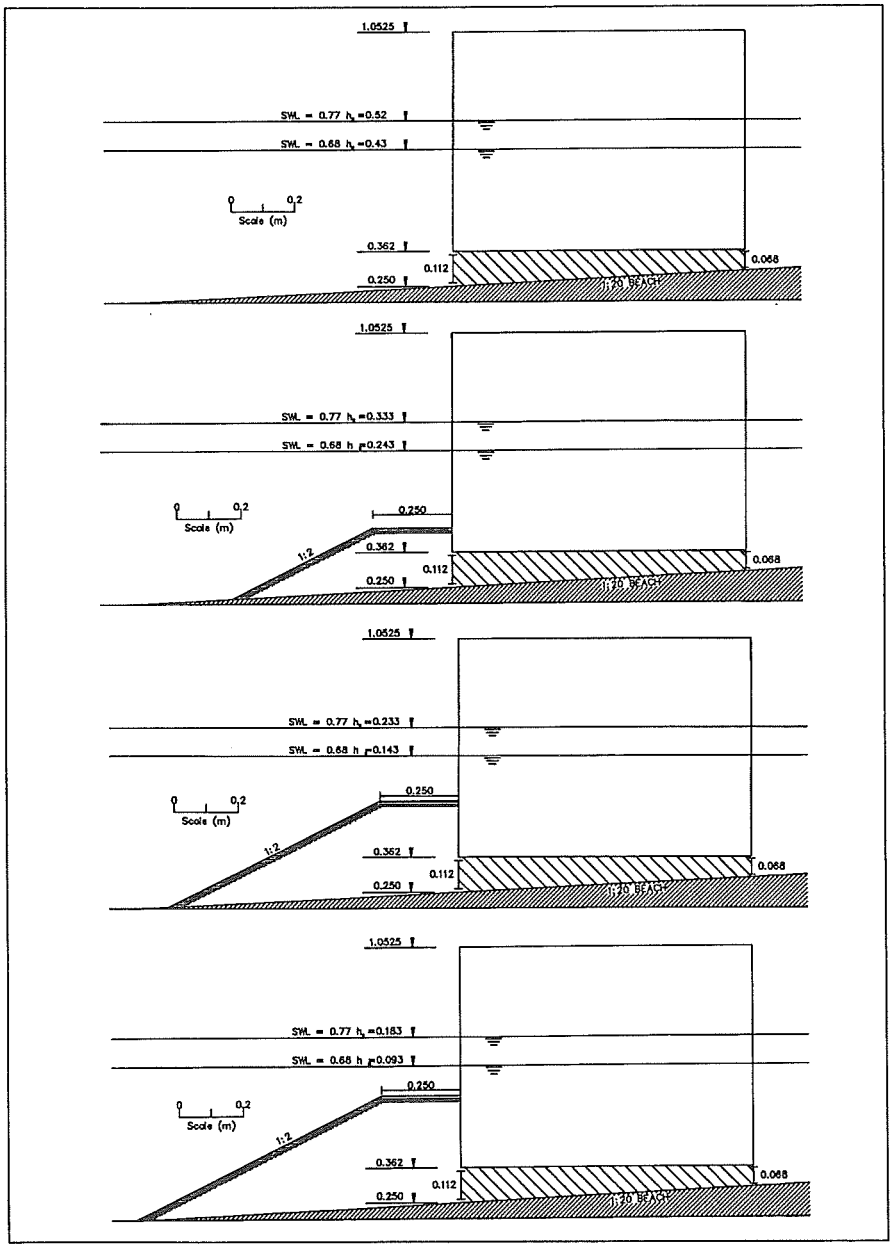

Figure 3.3 Cross-sections of test structures

The beach slope was maintained at 1:20 for this study, although a slope of 1:50 had been used previously for the 2-dimensional study. Comparison of the 2-d and 3-d test results under normal wave attack will determine the whether the approach bathymetry has any influence on the wave forces and occurrence of impacts on the caisson.

3.2 Design of tests

3.2.1 Test facility

The CRF wave basin shown in Figure 3.1 measures 54m by 27m, and operates with water depths between 0.3 and 0.8m at the paddles. An absorbing shingle beach constructed along the top of the test bathymetry reduced re-reflection of wave energy. The facility has large channels at each side which had been used on other studies to generate currents. When not in use during this study these channels proved effective at dissipating reflected wave energy.

The bathymetry in the basin had been formed by moulding concrete mortar. In deep water near the paddles, the bed was horizontal for

approximately 8m. The seabed then sloped upwards at 1:20 until it reached a level 0.67m above the basin floor. The bed was then horizontal at this level for 1m up to the basin wall. The shingle absorbing beach was placed in front of the basin wall, Figure 3.2.

Waves were generated by 72 multi-axis piston paddles. The paddles are controlled using software developed at HR Wallingford (HR WAVEGEN). This software enables either long crested regular and random waves, short crested random waves and oblique waves to be generated in the basin. The (normal direction) random wave signals are generated using a white noise filter technique with a single shift register, to match any wave spectrum that can be specified at 32 equal frequency ordinates. The oblique random wave signals are generated by the summation of sine waves specified at 48 equal frequency ordinates. JONSWAP wave spectra were generated for all of the tests. The nominal wave conditions summarised in section 3.2.3 were generated and measured in the deep water section of the basin. The wave conditions at the location of the caisson toe were measured during the calibration tests and are described in section 3.4.

3.2.2 Test structures

The four structures considered in this report and shown in Figure 3.3 were:

Structure 0	Test series 10,000	Vertical wall, toe of caisson at 0.25m, crest at 1.0525m.
Structure 1	Test series 1,000	Composite structure, berm height h_b=0.187, mound berm width B_b=0.25m, front slope 1:2.
Structure 2	Test series 2,000	Composite structure, berm height h_b=0.287, mound berm width B_b=0.25m, front slope 1:2.
Structure 3	Test series 3,000	Composite structure, berm height h_b=0.337, mound berm width B_b=0.25m, front slope 1:2.

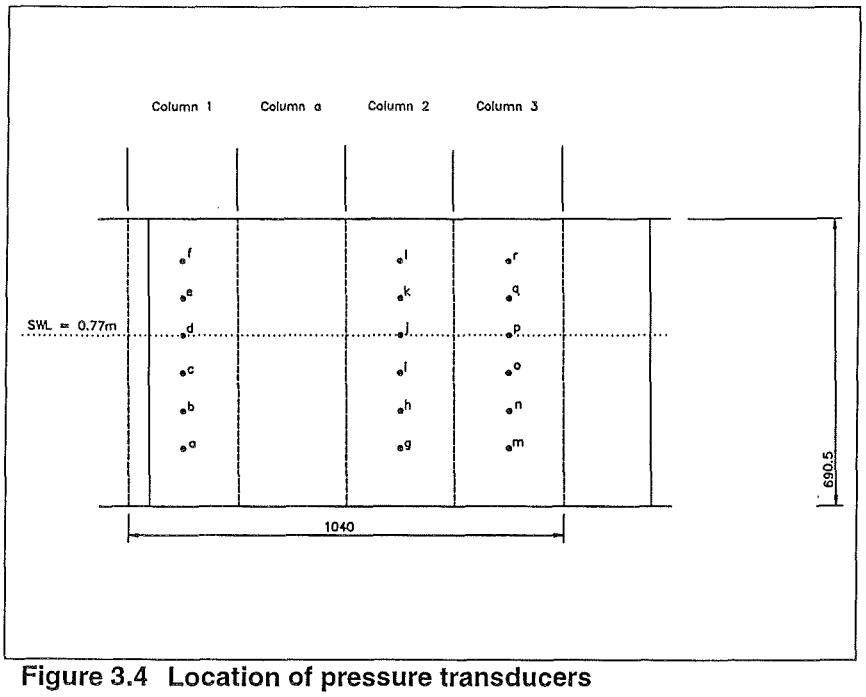

Figure 3.4 Location of pressure transducers

Structure 0 was a simple vertical wall, tested to measure wave forces against the simplest configuration. The composite structures were systematic variations on the vertical wall, designed to study the influence on wave forces of relative wave height H_{si}/d and relative mound size h_b/h_s and B_b/L_p.

The model caisson was formed as a box in marine plywood. To provide the correct crest height the caisson was secured to two beams anchored to a metal frame in the seabed. The small gap between the seabed and underside of the caisson was blocked with a timber plate to provide a continuous vertical face. The front face and underside of the caisson were stiffened with metal plates to provide enough rigidity to simulate a prototype concrete caisson.

Eighteen pressure transducers were installed on the front face of the caisson. These transducers were located in three columns, each with 6 transducers at different levels (Figures 3.4-3.5). The use of a hollow box enabled pressure transducer cables to run freely into the box, where they were bundled together, before transferring them from the test area to the logging equipment.

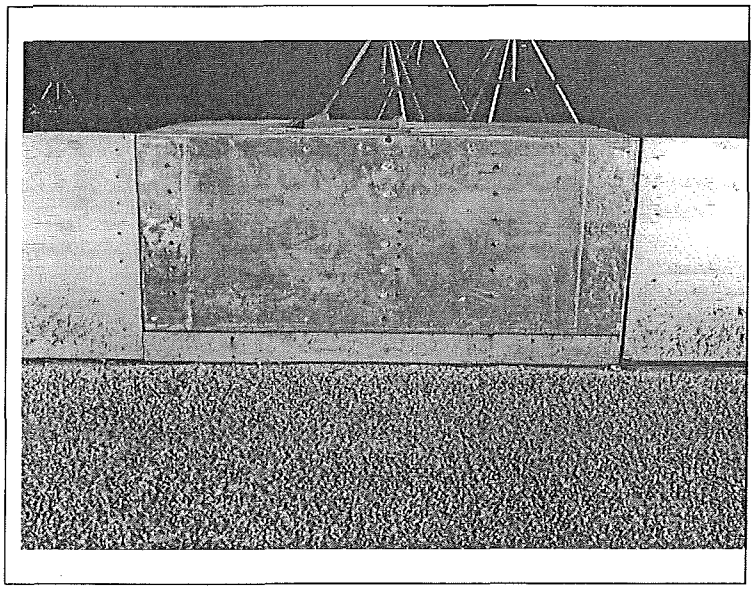

Figure 3.5 Photograph of test caisson

The rubble mound consisted of two rock gradings: the core (100 -150g) and the armour layer (1000 - 1200g). The berm and the front slope were formed in core material, to which two layers of armour were added.

3.2.3 Test conditions

A range of wave conditions at two water levels and four different directions were used for the model tests, in order to investigate the performance of the different structure types under different prevailing sea states. The wave conditions were chosen such that the influences of significant wave height, mean sea steepness and wave direction could be investigated separately, and direct comparisons could be made between the two different water levels. The wave directions tested were 0, 15, 30 and 45 degrees relative to the structure. The nominal wave conditions used are summarised in Table 3.1 below. All of the 150 conditions tested are listed in Appendix 1.

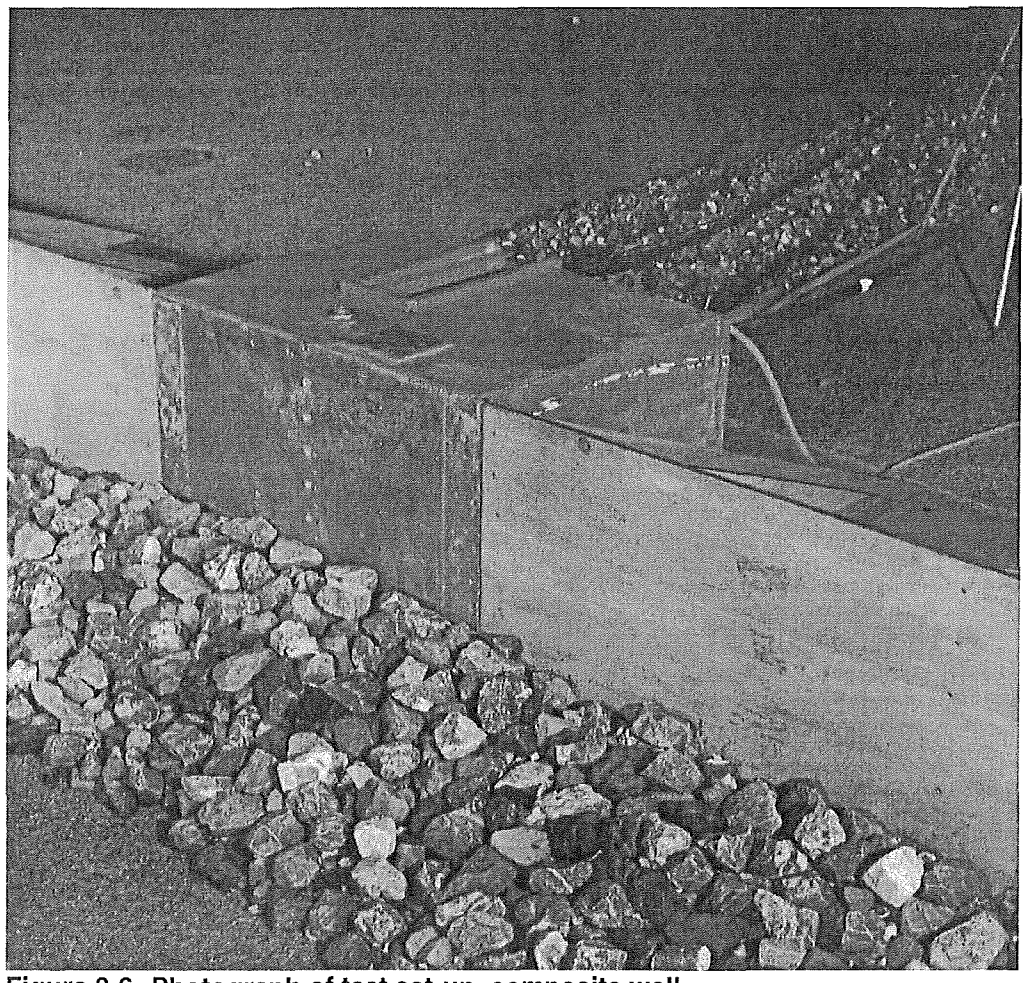

Figure 3.6 Photograph of test set-up, composite wall

Table 3.1 Nominal wave conditions

H_s(m)	s_m=0.02 T_m(s)	s_m=0.04 T_m(s)	s_m=0.06 T_m(s)
0.1	1.8	1.3	1.0
0.2	2.5	1.8	1.5
0.25	2.8	2.0	1.6

3.3 Instrumentation and test measurements

The main measurements made during these tests may be summarised as:

a) Instantaneous water levels used to determine wave height / period, using standard HR twin wire wave probes and logging modules;

b) Number of overtopping waves detected by 3 short wave probes mounted on the caisson crest;

c) Wave reflections derived by analysis of the output from an array of 3 wave probes in front of the test structure during normal wave attack;

d) Wave pressures on the front face of the caisson (3 columns of 6 transducers);

e) Video record of wave profiles observed from the side of the basin, together with a video record of waves recorded from above, suspended from the roof of the building.

Four computers were used during testing. The first computer was used for wave generation using HR WAVEGEN. On the second, data was acquired from all 18 pressure transducers and the 3 overtopping probes simultaneously at 400Hz using the DATS Software package. The third computer was used to record data from the wave probes (three offshore and three for reflections) through HR WAVES. The fourth computer, equipped with a re-writable optical device, was used to back-up pressure and wave data recorded on other computers.

Three different types of pressure transducers were employed on the front face of the caisson, they all exhibited the same characteristics and possessed similar calibrations. Eight transducers were by Control Transducers Model AB in the range 0 - 6 psi. The remaining pressure transducers were by Druck, 6 PDCR 810, 0 - 2.5 psi, and 4 PDCR 830, 0 - 15 psi.

Before testing commenced, all transducers were checked and calibrated. The transducers were set up so that 1m of (fresh) water head was equivalent to approximately 1 volt. With a range of 0-10 volts on the analogue to digital converter board, this ensured that all pressure signals that could be measured at high resolution would be recorded in 0-8 volts. The remaining range was available for any further over-load conditions up to a maximum of 10m head (a linear transducer response was assumed). A daily calibration check was used to ensure that the transducers functioned correctly.

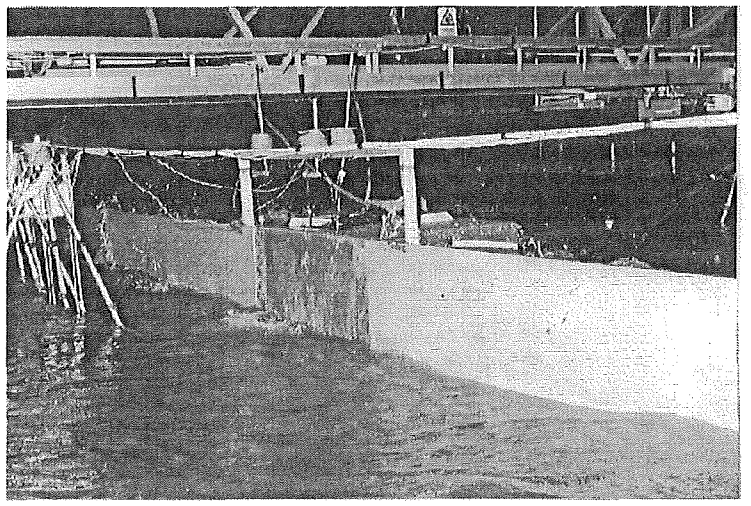

Figure 3.7 Photograph of test set-up (no waves)

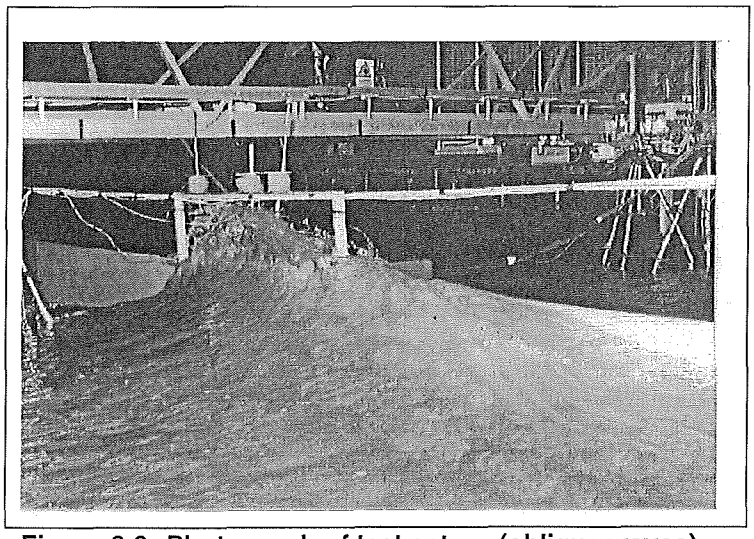

Figure 3.8 Photograph of test set-up (oblique waves)

3.4 Test and analysis procedures

Before the model caisson was installed, wave conditions at the position of the structure were measured during calibration tests. Measurements of water surface elevations were made using 6 twin wire wave probes, 3 located in deep water and 3 on the test beach where the model caisson was to be placed. Short sequences of about 300 waves were generated and incident wave conditions were determined using spectral analysis. Once the nominal wave conditions had been achieved, more comprehensive measurements were then made using longer sequence lengths of 500 waves, analysed using statistical methods. This ensured that extreme waves were reproduced correctly, and that the statistical distribution of wave heights was recorded. These longer wave sequences were then used during testing to ensure that extreme waves were correctly represented. Incident and reflected wave conditions were measured during normal wave attack using 3 twin wire wave probes, located close to the structure on its seaward side. The overall reflection coefficient, C_r, was determined by summing energies in each frequency band for individual test conditions. A table detailing each of the 150 conditions tested, giving the calibration measurements, is given in Appendix 1.

Pressure data from the 18 transducers were acquired at a rate of 400Hz, un-filtered. Data were acquired continuously for all channels throughout each test (typically 500 waves). The data files generated were extremely large, even in multiplexed binary format, and had to be expanded by de-multiplexing prior to analysis. Once de-multiplexed, all files were passed through a preliminary analysis process, from which selected data were further processed.

The first problem in the analysis of the data was to reduce the files to a manageable volume. The first part of the analysis identified those parameters to be recorded for each impact "event", and thus reduce the volume of data to be processed.

Measurements of wave pressure were processed using a program by Centurioni et al (1995) adapted for this study by McConnell, see Appendix 2. The main activity of this program was to recognise each wave "event" from the pressures signals so that the program finds the (rapid) pressure rise that may be taken to mark the beginning of each wave impact. The definition of an "event" is given in the Appendix. At its simplest, it is generally expected that a single wave will cause a single force (or pressure) event. The start of an event may be defined as the wave starts to run up the wall. The end of the event will be given by the start of the next event. In practice, "event" recognition is not so simple, and a complex series of tests have to be coded into the analysis program to define thresholds, start and end points. In general in this report, events will be defined by force, but in other work they may be defined by pressures.

Another section of the program then checks if the signal is decreasing and falls below an appropriate threshold which is a function of the zero level. When this double condition is verified, the program starts again to look for a new event so that, if a signal has two peaks or is stepped, the program will only record a single start of event. The event definition is checked only for the record from the still water level transducer. First events in any record are always discarded because the measurements might begin within the event rather than at its start.

The algorithm used for the event definition calculates 2 running averages, and their ratio. When this ratio is greater then 1.1 for $(T_m/10)*400$ consecutive times, the program recognises an event and transfers control to another section. The program later seeks an "end of event", after which the program searches for the next event.

After all events have been identified, the program reads through all the channels and the peaks of pressure are detected for all transducers. For each event and for each transducer, the routine finds the time interval between the pressure peak and when the signal is 20% of the peak (Δt). Before moving to the next event, the program derives the main output parameters: the horizontal force and the overturning moments. Pressures on front face are summed using the trapezoid rule. The program also records the maximum pressure for each event, and for each channel.

The forces and moments acting on the (model) caisson at each timestep were calculated from the pressure measurements using simple numerical integration. The positions of the transducers did not cover the full height or width of the caisson, so some interpolation and indeed extrapolation were necessary. The trapezium rule was chosen in preference to the staircase method or Simpson's rule since it permits flexibility in the spacing of the intervals, yet gives results which are in good agreement with analytical integration methods. Integration by the staircase method tends to over-estimate forces and moments where there is a high local pressure since it assumes that pressure acts over the whole area between the measurement points. Simpson's rule can provide additional accuracy in curve integration, but in this case there is nothing to suggest that the accuracy would be increased as the form of the distribution is unknown. Simpson's use of a parabolic distribution over three adjacent points may in fact reduce the accuracy in some cases.

Forces on the three columns of transducers were combined to investigate the variability of the extreme horizontal forces along the caisson. Since column "a" was not equipped with instrumentation, the pressures measured on columns 1 and 2 were averaged to find a value for this column at each timestep. The maximum wave forces on each column were found for each force event. To simulate the effect of increasing the caisson length, the maximum forces for each timestep were averaged over combinations of adjacent columns. The maximum force for each combination of columns was then found for each force event. The combinations of columns used and the caisson lengths that they represent are given in Table 3.2. In some instances more than one combination was used to represent a given caisson length.

Table 3.2 Combinations of columns of transducers

Number of caissons n (-)	Caisson length L_c (m)	Adjacent column combinations		
0	0	1	2	3
1	0.26	2, 3		
2	0.52	1, a, 2	a, 2, 3	
3	0.78	1, a, 2, 3		

The maximum wave forces for each column and each event were ranked in order of magnitude. The forces above the 1/250 non-exceedance level were averaged for each column and each combination of columns to give values of $F_{h1/250}$. Where more than one combination was used to represent a given caisson length the average of the value of $F_{h1/250}$ was used. To estimate the (expectation value of the) extreme wave force on an infinitely short length of caisson, the average of $F_{h1/250}$ over the three columns was calculated. The extreme force over each caisson length L_c was divided by the extreme force over an infinitely short length to demonstrate the variation of the force with increasing caisson length: $C_{Fh} = F_{h1/250\,(n)} / F_{h1/250\,(0)}$, where n is the number of caissons.

When the caisson length is zero, n=0, then $C_{Fh} = 1$, indicating that there is no variation in the extreme wave force. It will however be shown later that highly variable values of $F_{h1/250}$ may lead to values of C_{Fh} which exceed 1.

3.5 Data handling, archiving and initial processing

The data collected during the series of tests described in this report were logged at 400 Hz as voltage time series on a 48 channel PC (although only 21 channels were used for this study).

There were several problems associated with recording and analysing data using this method due to the volume of data being recorded, and hence the time taken to store and handle it. Typically data were recorded for 500 waves, but a few tests were reduced to 200 waves due to wave paddle failure. A small

group of tests were repeated with a much longer time sequence, of 2000 waves, to study the influence of duration upon the distribution of peak force events.

The data were initially written to the computer hard disk in multiplexed binary format, occupying 20 to 40 Megabytes of hard disk space for a 500 wave test, dependent upon wave period. Before analysis, it was necessary to de-multiplex each acquisition data file into 18 individual binary files of voltage time series for each pressure transducer, and 3 files containing the wave overtopping data. The de-multiplexed data files then occupied twice the disk space of the acquisition files.

Hard disk space on the acquisition computer was limited, and it was only possible to store one or two data acquisitions on the computer before it was necessary to down-load them to another storage device. Testing, therefore, had to be interrupted regularly in order to transfer the data files. These files were transferred from the logging computer to the data storage computer via a local network in the CRF. The multiplexed files were written to re-writable 650 Megabyte optical disks (OD) for short term storage and transfer to the HR network. The data files were then de-multiplexed prior to analysis. Both the multiplexed and de-multiplexed files were written to 650 Megabyte compact disks (CD) for long term storage. For security reasons it was necessary to make duplicate copies of each multiplexed data file. The results from the analysis program have also been stored as spreadsheets on the compact disks. The data handled in this project may be summarised:

- 120 random wave tests;
- 30 regular wave tests;
- 4000 Megabytes of multiplexed data files;
- 8000 Megabytes of de-multiplexed data files;
- 600 Megabytes of initial stage analysis spreadsheets;
- 200 Megabytes of second stage analysis spreadsheets;
- 30 CD Roms.

4. ANALYSIS OF WAVE FORCE / PRESSURE RESULTS

4.1 Distribution of wave forces

Initial analysis of wave forces derived from the pressure signals concentrated on distinguishing between pulsating and impacting conditions. The analysis followed essentially the same procedures used in the 2-d analysis in SR 443 in which probability distributions of force summed from a column of pressure transducers were plotted on Weibull axes. On these particular axes, the Weibull probability axis uses exceedance probability P, expressed as a double logarithm, plotted against the (logarithm of the) wave force. The graphs are not intended for scaling, but simply to demonstrate the form of the probability distribution, and to provide estimates of the degree of wave impacting onto the wall.

In this presentation, any sustained departure of forces above the Weibull line was taken as indicating wave impacts. Example distributions for simple vertical walls under normal wave attack are shown in Figures 4.1 - 4.6, and are discussed below. Whilst three columns of transducers were used in testing, for simplicity most of the force distributions discussed here have been averaged to give a single distribution for each test condition.

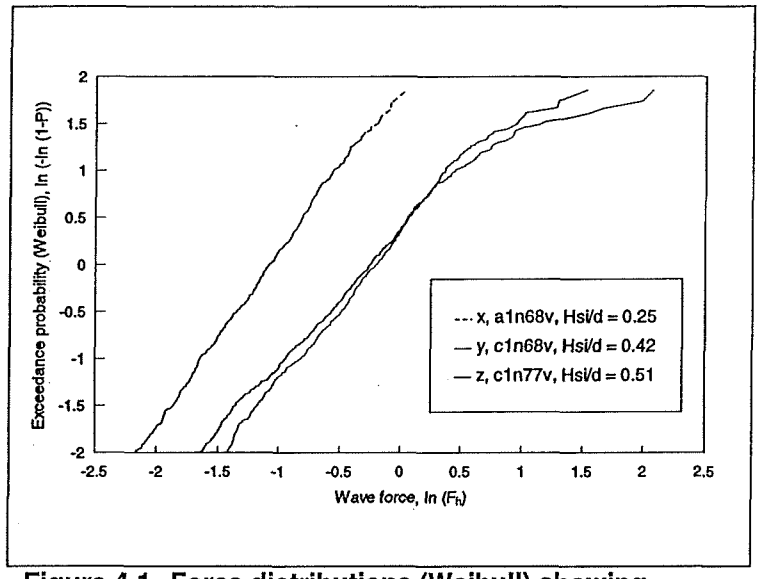

Figure 4.1 Force distributions (Weibull) showing influence of wave height and water depth

Again following the procedure of SR 443, the percentage of impacts (P_i) was calculated for each test. This was found from the non-exceedance probability on the force distribution graph at the point where the wave forces showed a sustained departure from the Weibull line. Where the extreme forces followed the Weibull line, it was deemed that pulsating conditions had occurred throughout the test and, so, $P_i = 0\%$.

The form of the distributions was similar to that seen in the 2-d study, but the distributions of forces in the 3-d tests were generally less close to the ideal Weibull than in the 2-d tests. Identification of P_i from these distributions was therefore a little less certain than in the previous study, but generally gave reliable results. Where there were important differences between the three columns, the number of breaking waves was found from the video record of the tests.

In the rest of this section selected tests are discussed to identify various trends. Later, more detailed analysis of occurrence of impacts (Section 4.2) and of extreme forces (Section 4.3) are discussed.

4.1.1 Influence of wave height and water depth

As seen in SR 443, the shape of the probability distributions of forces changes as the relative wave height H_{si}/h_s or H_{si}/d is increased, generally increasing the percentage of impacts, P_i. This is illustrated for values of H_{si}/d = 0.25, 0.42 and 0.51 in Figure 4.1.

For H_{si}/d=0.25, labelled as line x, a good Weibull fit is found, with no significant departure from the straight line for extreme wave events. It was therefore deduced that no impacts had occurred, and so P_i=0%. For line y, the wave height was increased to H_{si}/d=0.42. The increase in overall forces is shown by displacement of the force line to the right up the force axis. At the upper end of the line, the extreme forces tended to deviate from the straight line which indicates that impacts were occurring above an exceedance probability of 3%, so $P_i = 3\%$.

For the last line, the wave height was maintained, but the water depth was lowered to H_{si}/d=0.51. Although the general level of forces on the caisson did not change significantly, the departure from the straight line started at a greater exceedance probability giving $P_i = 9\%$, and increased extreme forces.

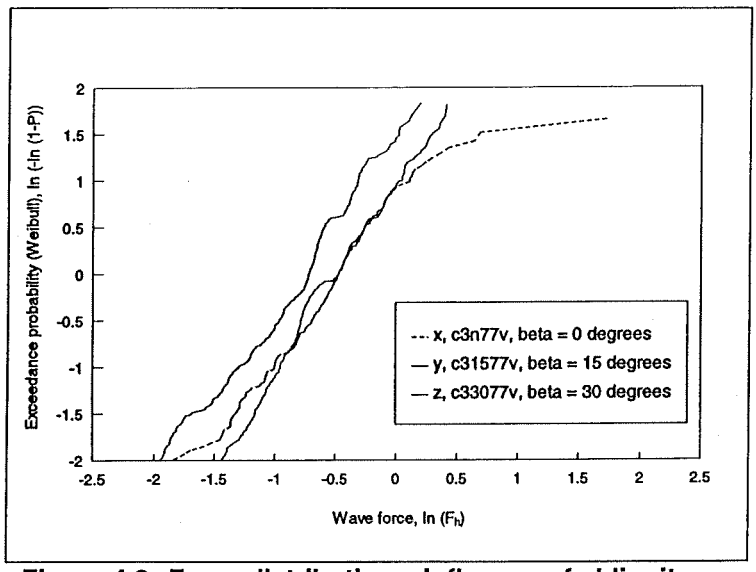

Figure 4.2 Force distributions, influence of obliquity

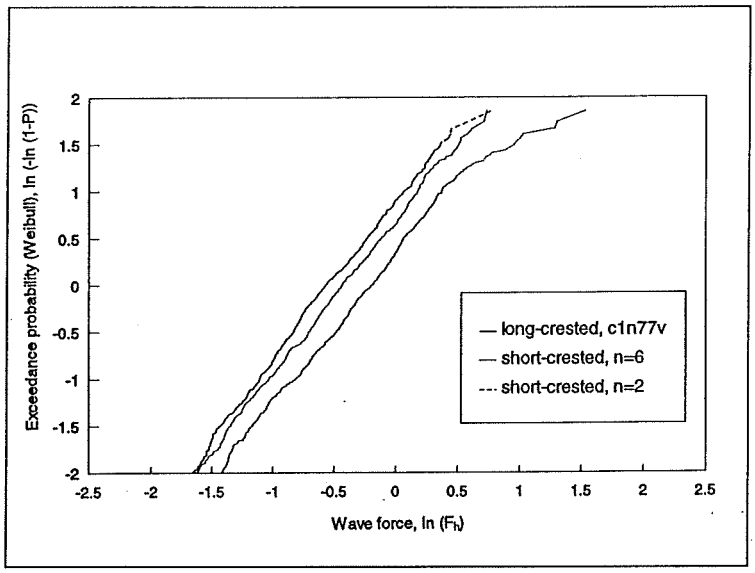

Figure 4.3 Influence of wave spreading

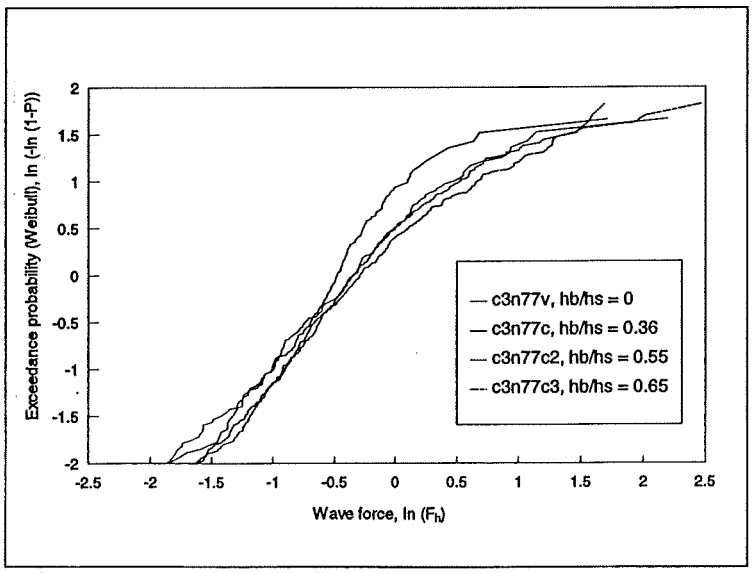

Figure 4.4 Influence of rubble mound

4.1.2 Influence of wave obliquity

Any obliquity of wave attack was expected to reduce wave forces overall, and particularly to reduce the occurrence of impacts. These processes are illustrated in Figure 4.2 where forces for waves of $H_{si}/d = 0.53$ are presented for $\beta = 0°$ (line x), $\beta = 15°$ (line y) and $\beta = 30°$ (line z). The occurrence of impacts reduces markedly from $P_i = 11\%$ at $\beta=0°$ to $P_i = 0\%$ at $\beta=15°$ and 30°. The overall level of horizontal force decreases with increasing obliquity from $\beta=0°$ to $\beta=15°$ as shown by the reductions in $\ln(F_h)$ over the upper part of Figure 4.2, but a similar reduction from $\beta=15°$ to $\beta=30°$ is not so clear. This effect may have been modified by the slight changes in incident wave heights between the three conditions here, but this will not invalidate the main conclusion.

4.1.3 Influence of wave spreading

Increasing wave spreading also reduces wave forces and occurrence of impacts. Wave forces under three conditions of increasing wave spreading, $n \rightarrow \infty$, $n = 6$, $n = 2$, are shown in Figure 4.3. The occurrence of wave impacts decreased from $P_i=3\%$ to $P_i=0\%$, with increased wave spreading. The overall forces are also reduced under this test condition, as shown by the reduction of $\ln(F_h)$.

Although these were nominally the same wave conditions, the incident wave height measured in the model varied between the three tests, from $H_{si}/d=0.32$ to 0.42. The reduction of P_i and the overall forces may, therefore, be due in part to the reduction of H_s rather than to the change in the wave spreading. In Section 4.2 the effect of short-crested waves will be investigated further.

4.1.4 Influence of rubble mound

It was shown in the 2-d study reported in SR 443 that the addition of a rubble berm to form a composite breakwater may increase the occurrence of impacts. This effect is again illustrated in Figure 4.4 although the trends at extreme exceedance were less clear than seen in the 2-d tests.

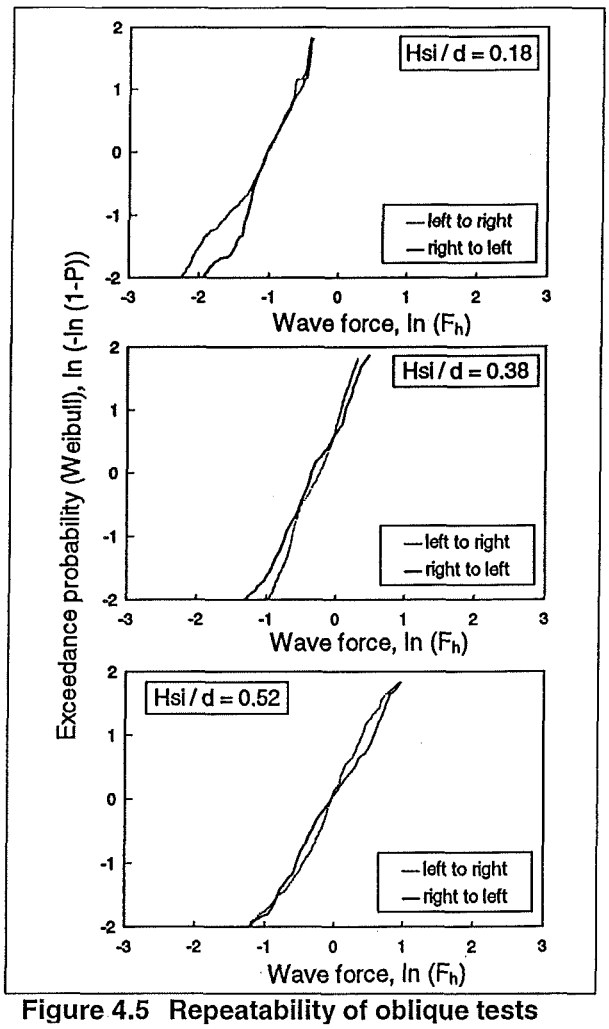

Figure 4.5 Repeatability of oblique tests

4.1.5 Repeatability of force distributions

In the previous 2-d study, considerable effort was spent to check tests for repeatability and consistency. In this study, the results of initial tests for normal wave attack with long-crested waves have been compared with 2-d results in earlier section 4.1. Further tests were also run to check consistency of waves and measured forces under oblique conditions. Selected tests for β = 15° were repeated with waves from the opposite side of the basin. Examples for wave conditions similar to those in Figure 4.1 are shown in Figure 4.5. The extreme forces from both directions, left to right and right to left, were generally similar with the maximum difference between extreme forces being about 10%.

4.1.6 Influence of test length

Selected tests were re-run for 2000 waves as well as for 500 waves to explore the effect of test length on reliability of extreme force measurements. The distribution of extreme forces for low values of H_{si}/d showed close agreement between 2000 and 500 waves, Figure 4.6,. Forces for greater relative wave height showed differences over the upper part of the non-exceedance range. For H_{si}/d = 0.38 and H_{si}/d = 0.52, results for 2000 waves showed greater extreme wave forces with impacts in the 2000 wave tests, where 500 waves only gave pulsating waves at the same exceedance level.

Where the force distribution is extended to the greater non-exceedance levels which were measured in the

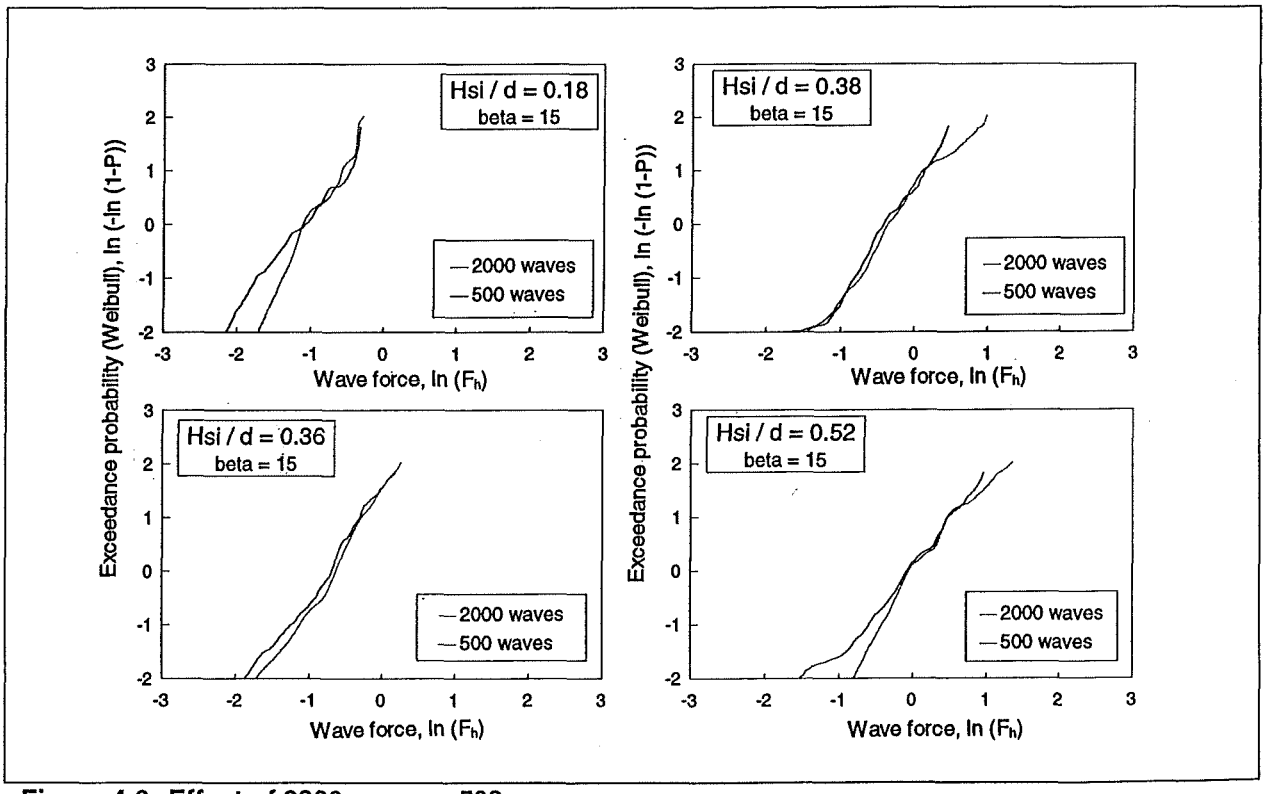

Figure 4.6 Effect of 2000 waves v 500 waves

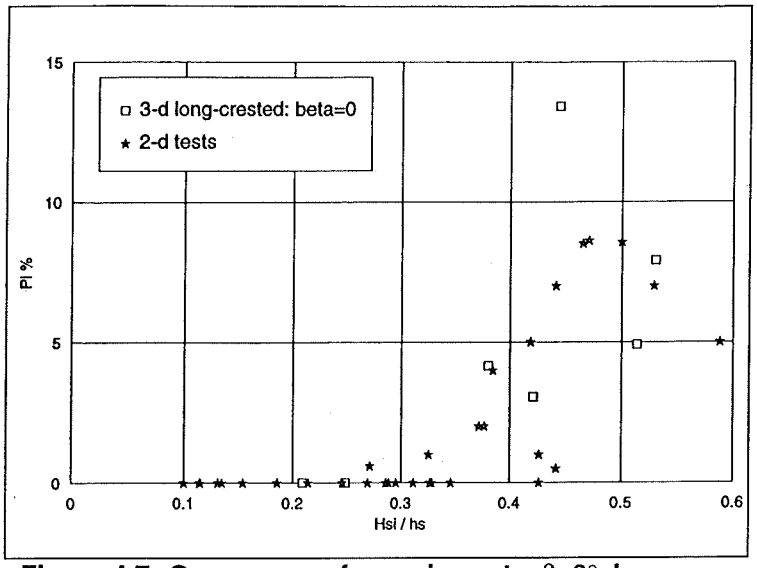

Figure 4.7 Occurrence of wave impacts, β=0°, long-crested, compared with 2-d results

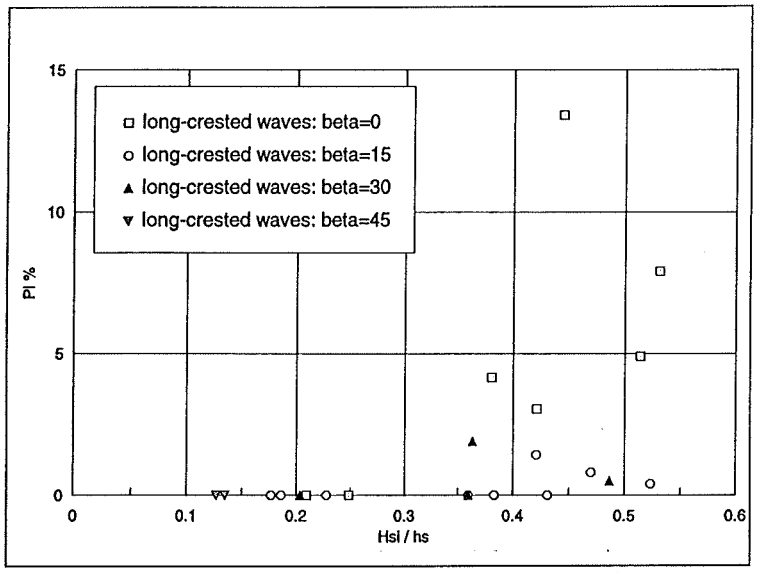

Figure 4.8 Wave impacts, oblique long-crested waves

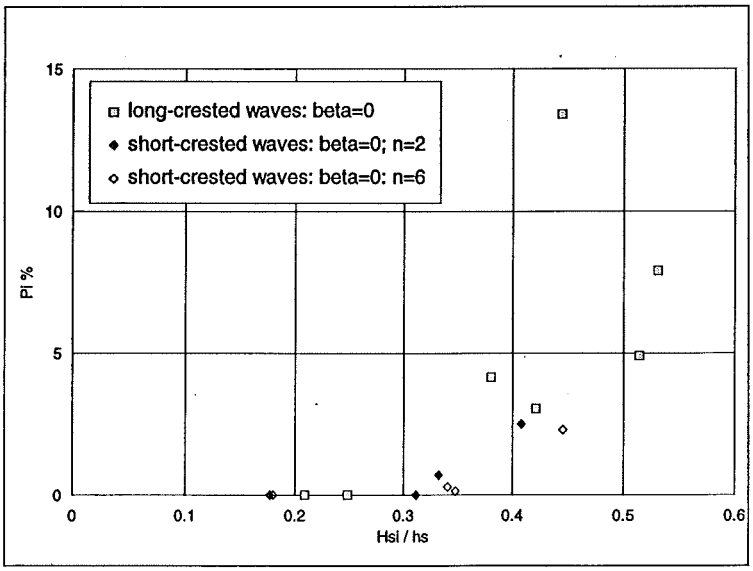

Figure 4.9 Wave impacts, short-crested waves

2000 wave tests, the forces are up to 60% larger than the extreme forces measured in the 500 wave tests.

In part these differences are not unexpected. The relative wave height for both these tests is in excess of the impact threshold of H_{si} /d = 0.35 which was identified in the 2-d analysis (Allsop et al., 1996). Beyond this threshold it was found that impacts were likely, but it was possible that pulsating wave conditions would persist. These results suggest that future studies should use durations greater than 500 waves, perhaps 1000 or 2000, and that repeat tests may be needed to identify natural variability of impacting forces.

4.2 Occurrence of wave impacts

Analysis of occurrence of impacts in this study is again principally conducted using graphs of P_i against H_{si}/d. In analysis of the 2-d tests in SR 443, wave impacts occurred where $H_{si}/d>0.35$. This limit is rather lower than the rule of thumb for wave breaking over shallow bed slopes given by $H_{si}/d=0.55$, but it is likely that a few waves in the distribution will start to break below $H_{si}/d=0.55$.

Given that the upper few waves in a distribution may be approximately 1.8 to 2 times H_s, and that limiting conditions for single waves over shallow slopes is $H_{max}/h_s=0.78$, the limit for the onset of breaking of $H_{si}/h_s=0.35$ appears reasonable.

4.2.1 Impacts on vertical walls

Normal wave attack

Average percentages of impacts, P_i over the three columns on the plain vertical wall are plotted against relative wave height, H_{si}/d in Figure 4.7 against data for 2-d study. For normal wave attack on vertical walls, the results are essentially similar to those in SR 443, suggesting that the use of the 1:20 bed slope in the CRF has not changed the breaking behaviour significantly. In particular, the 3-d results confirm that wave impacting starts as the relative wave height H_{si}/d exceeds 0.35.

Oblique wave attack

The occurrence of impacts under oblique wave attack is shown in Figure 4.8 where P_i is plotted against H_{si}/d for $\beta=0°$, $\beta=15°$, $\beta=30°$ and $\beta=45°$. These results illustrate the rapid decrease in wave impacting as obliquity increases from $\beta=0°$ to $\beta=15°$. At $\beta=30°$ and $\beta=45°$ no impacting occurs. This reduction may be important, since in the 2-d study it was found that a decrease in the percentage of impacts, particularly to $P_i=0\%$, indicated significant reductions in extreme wave forces on the structure.

Under normal wave attack, and for small obliquities, the onset of wave impacting was confirmed to be $H_{si}/d = 0.35$.

For more oblique attack, $15° < \beta \leq 30°$, this may be increased to $H_{si}/d = 0.40$. For very oblique attack, $\beta>30°$, is seems very unlikely that wave impacting will occur. This is consistent with the impulsive breaking criteria given by Goda (1985) in which wave obliquity greater than $\beta=20°$ presents "little danger" of impulsive pressures occurring.

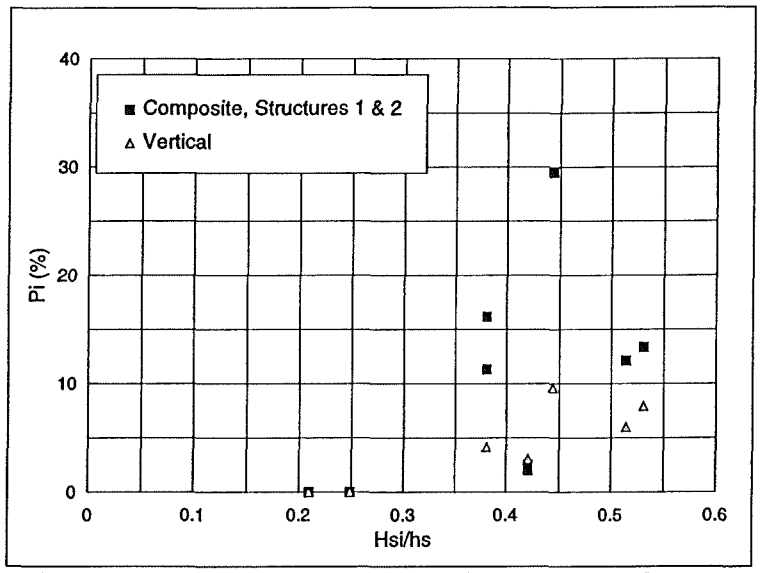

Figure 4.10 Wave impacts, composite, low mounds

Short-crested wave attack

The occurrence of impacts under short-crested wave attack is shown in Figure 4.9 where P_i is plotted against H_{si}/d for $n\rightarrow\infty$ (long-crested waves), and for increasing degree of spreading n=6 and n=2.

At low relative wave heights, $H_{si}/d < 0.35$ wave spreading causes a small increase in impacts from $P_i = 0\%$ to $0\%<P_i<1\%$. Although this is a small absolute increase in P_i it may be significant since even a small number of impact waves may increase extreme forces on the wall. This increase may arise from greater spatial and temporal variability of wave profiles under short-crested conditions.

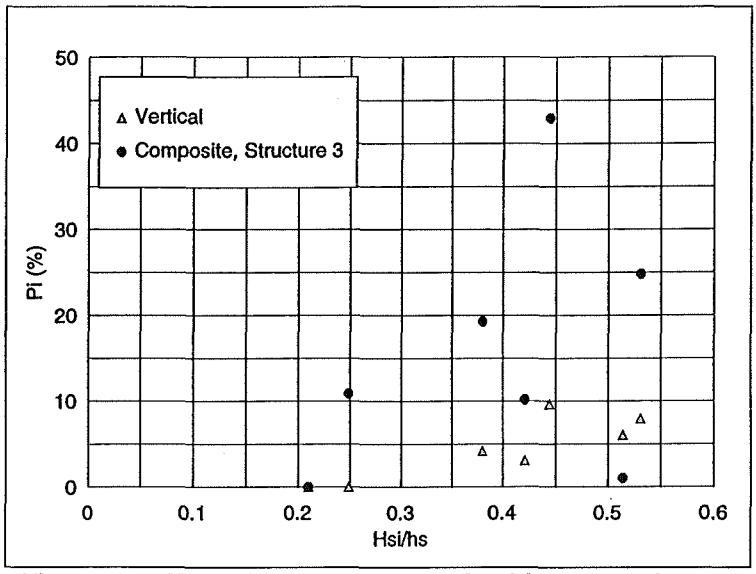

Figure 4.11 Wave impacts, composite, high mound

4.2.2 Impacts on composite walls

Normal wave attack

In the 2-d study reported in SR 443, the composite structures were divided into low mounds defined by $0.3 < h_b/h_s < 0.6$; and high mounds $0.6 < h_b/h_s < 0.9$. This allowed categorisation of the behaviour of the wave forces, and these categories are retained in this report. Structures 1 and 2 in this study had low mounds, $(0.35 < h_b/h_s < 0.55)$, whilst Structure 3 had a high mound $(0.65 < h_b/h_s < 0.73)$.

The influences of the rubble mounds on wave impacts , P_i are plotted against relative wave height in front of the rubble mound H_{si}/h_s in Figures 4.10 – 4.11. Comparison with Figure 4.7 shows that composite structures again sustain more wave impacts, sometimes substantially so, much as shown in SR 443.

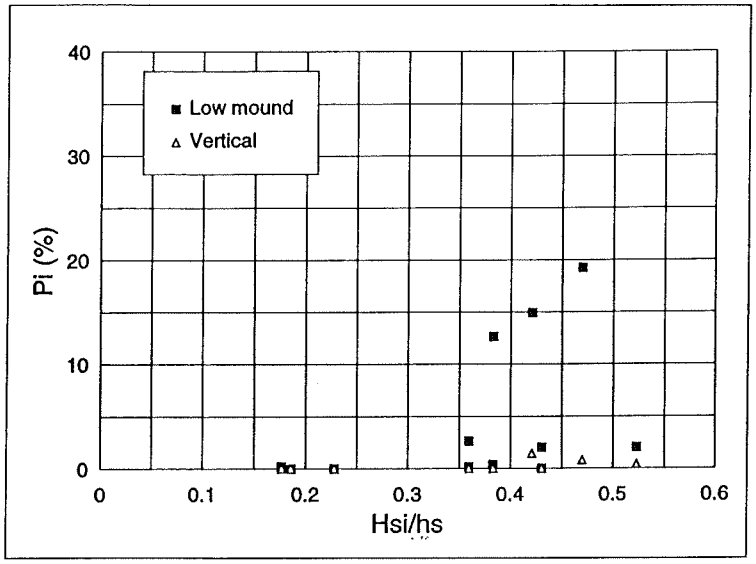

Figure 4.12 Wave impacts, composite, low mound, β=15°

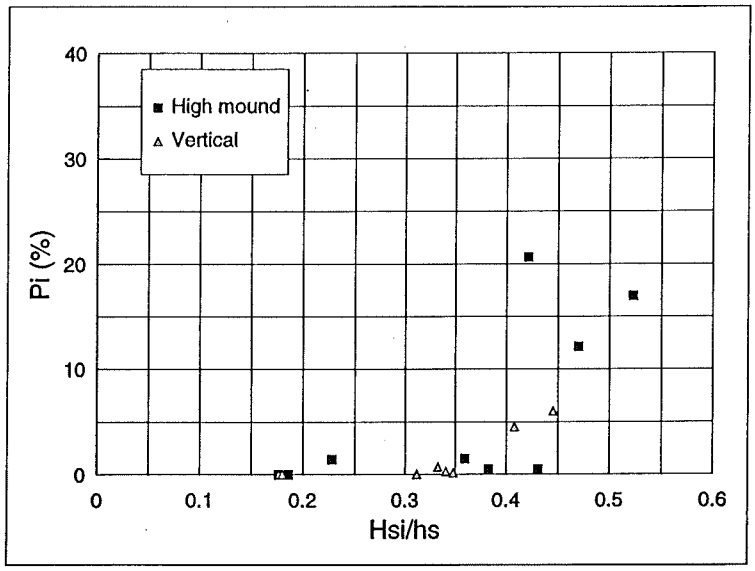

Figure 4.13 Impacts, composite, high mound, β=15°

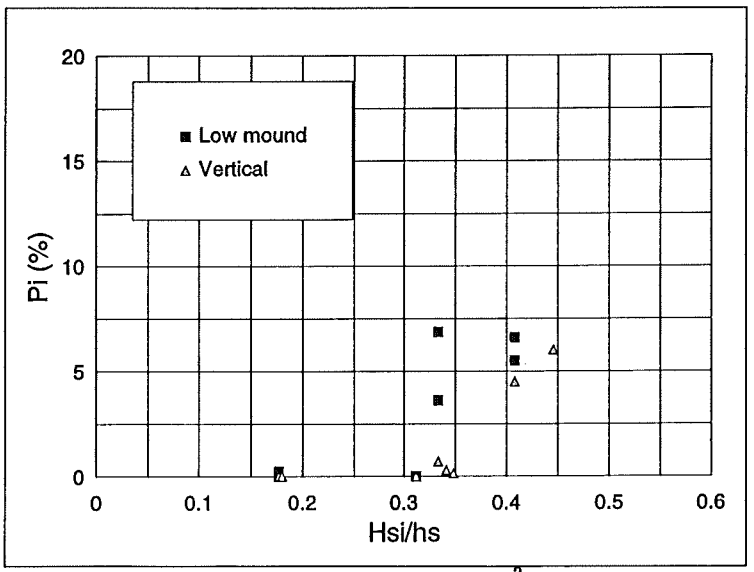

Figure 4.14 Composite low mound, cos^2 spreading

Addition of the mound also influences the onset of wave impact breaking onto the wall, inducing impacts at a lower value of wave height relative to water depth in front of the structure (H_{si}/h_s = 0.2). The value of relative wave height to mound depth H_{si}/d, varies for each structure since the depth over the mound decreases as height of mound increases: for structure one H_{si}/d= 0.28, for structure two H_{si}/d=0.40 and for structure three H_{si}/d=1.05.

Oblique wave attack

As for the simple vertical walls discussed in section 4.1.1 above, wave obliquity again reduces the occurrence of impacts, although the effect is not always quite as clear as for the vertical wall. For a low mound wall and wave obliquity of β=15°, shown in Figure 4.12, there are very few significant impact events, although there are a few more for the high mound structure, Figure 4.13.

For greater obliquities, β =30 and 45° there were no impact events for the conditions tested. It should be noted that this was only for low mounds (h_i/h_s < 0.6), but the significant reductions seen already for oblique attack on low mounds suggest that the occurrence of wave impact events on high mounds is most unlikely for strongly oblique waves.

Short-crested wave attack

The influence of wave spreading is also less clear for composite walls (Figure 4.14). There was possibly some slight reduction in the proportion of impacts, P_i for the smallest mound, but results for Structure 2 with a higher mound showed no specific trend.

Whilst all of the short-crested test conditions for vertical walls caused wave impacting, there were some conditions on the composite walls which showed pulsating conditions throughout testing.

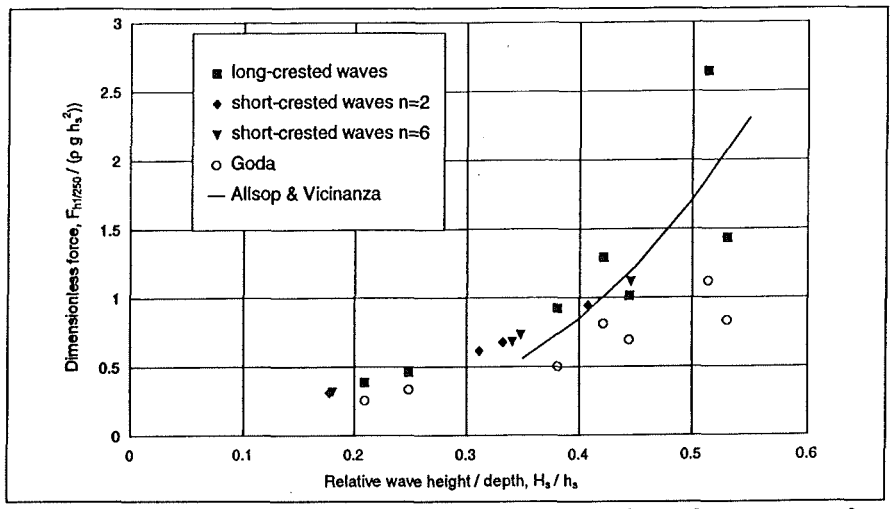

Figure 4.15 Dimensionless forces, vertical wall, β=0°, long-crested

4.3 Loads on vertical walls

4.3.1 Normal wave attack

Wave forces at 1/250 exceedance level were calculated from pressures for each column of transducers. For analysis of overall forces under normal long-crested wave attack, these values were then averaged over the three columns and in Figure 4.15 are presented as values of $F_{h1/250} / \rho g h_s^2$ against H_{si}/h_s. For this initial analysis, no account is taken of the effect of caisson length.

Forces in the 3-d study tended to be slightly greater than those from the 2-d study, but, given the ranges of values measured by the three columns, the sets of data are comparable. In the previous 2-d study it was found that Goda's method generally gave conservative results for pulsating wave conditions, but under-estimated forces under impact conditions. Thus where $H_{si}/d<0.35$, it was suggested that Goda's method was used, but for $H_{si}/d>0.35$ a new prediction developed by Allsop & Vicinanza (1996) was proposed:

$$F_{h\,1/250} / (\rho g d^2) = 15\,(H_{si} / d)^{3.134} \qquad (4.1)$$

For pulsating conditions, $H_{si}/d < 0.35$, there is reasonable agreement with Goda's predictions, and with results from Franco et al for $H_{si}/h_s=0.20$. For larger relative wave heights, the measured forces again exceed those predicted by Goda's methods, but generally lie either side of the prediction line by Allsop & Vicinanza shown in Figure 4.15.

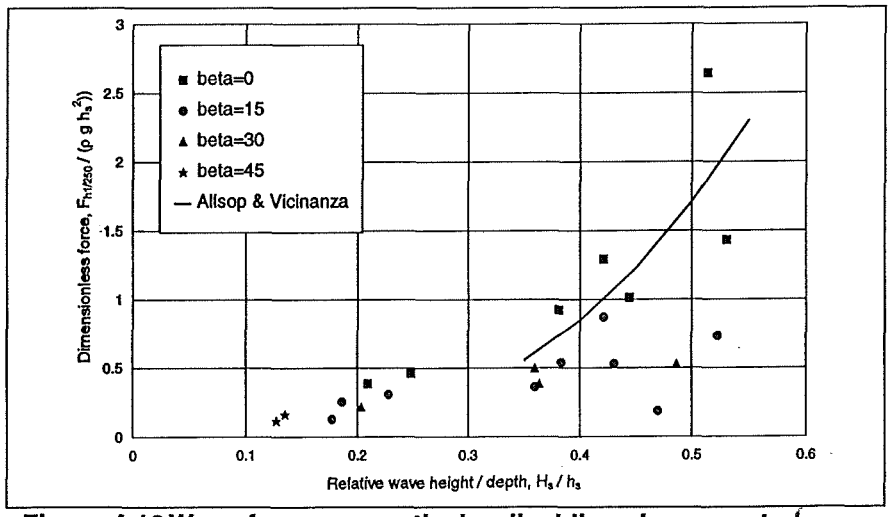

Figure 4.16 Wave forces on vertical wall, oblique long-crested

4.3.2 Oblique waves

As expected from previous work discussed in Chapter 2, and from the analysis of wave impacts discussed above, the effect of oblique attack is generally to substantially reduce impact loads, with rather smaller reductions for pulsating loads.

Forces measured for β= 15°, 30° and 45° are compared in Figure 4.16 against forces for normal wave attack, β= 0°. As expected, the most significant reductions in measured forces are given for $H_{si}/h_s> 0.4$, where Allsop & Vicinanza's simple equation gives reasonable estimates for impact waves under normal attack, but substantially over-estimates loadings under oblique conditions.

4.3.3 Short-crested waves

Measurements of average forces at 1/250 level for short-crested wave attack are compared with those already discussed for long-crested waves in Figure 4.17. These results show that the effect of wave spreading under normal wave attack is not significant in reducing wave forces, even though the component

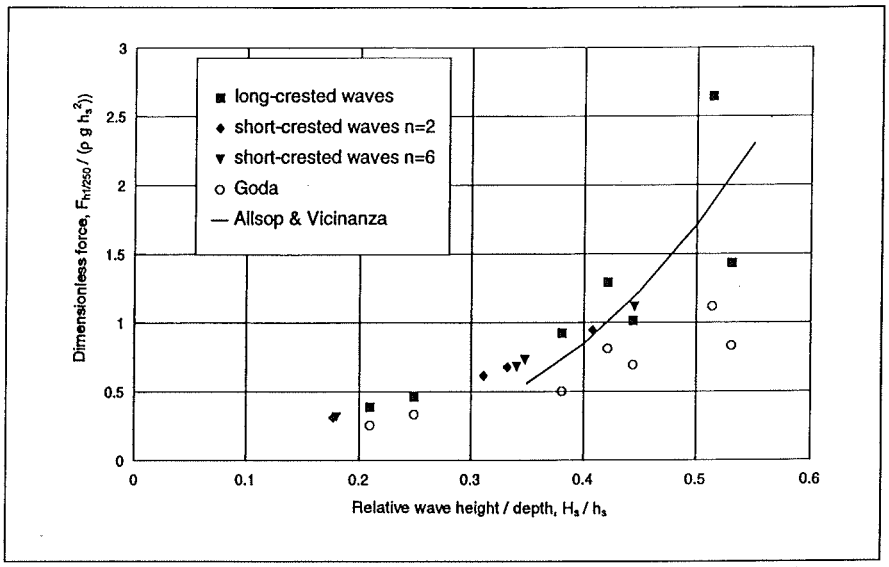

Figure 4.17 Wave forces on vertical wall, normal short-crested

of force perpendicular to the structure might have been expected to reduce. Nor is there any significant difference in measured forces for narrow or wide spreading.

4.4 Variability of forces

Up to this point in the analysis, all forces have been calculated by averaging instantaneous values over the 3 columns of transducers. It is however possible to estimate variations of peak force by comparing results from the 3 columns of transducers using three different methods, each giving less averaged values:

a) from the force averaged across all three columns, calculated at each timestep;
b) from peak forces on each column, averaged event by event, but not necessarily at precisely the same point in time;
c) from peak forces on any individual column, irrespective of event, or timestep within the event.

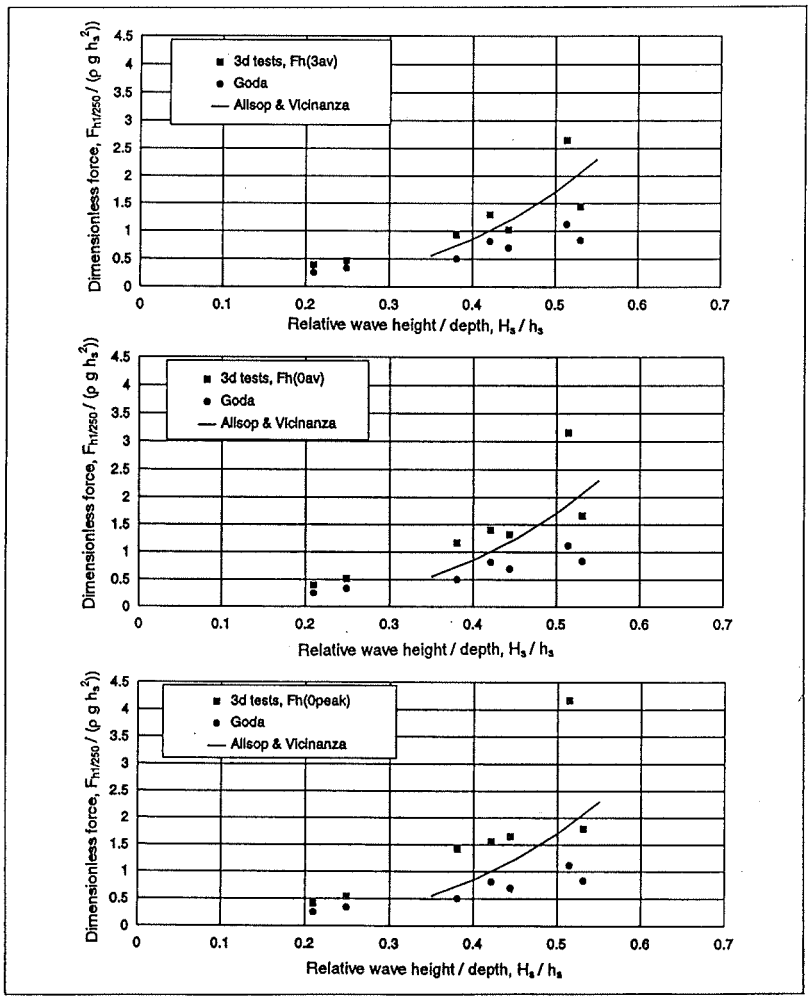

Figure 4.18 Wave forces as peak (local), or averaged

Most analysis of model test results, and hence development of prediction methods have been based on forces averaged by methods a) or b). These average values are necessarily smaller than the peak (local) values calculated using method c). Some estimates of increase in "local" force may therefore be derived from comparison of these values, plotted as dimensionless forces in Figure 4.18.

As expected, these comparisons show consistent increases in $F_{h1/250}$ with reduced averaging, from methods a) in the top part of Figure 4.18, down to the peak individual values in c).

The simple formula by Allsop & Vicinanza (1996) gives reasonable estimates of forces averaged over typical caisson widths of 10-20m, but under-estimates the "local" force over a single narrow strip, even for normal long-crested wave attack.

Peak values in c) have been compared with average forces in a) as $F_{h(peak)}$ / $F_{h(av)}$ plotted against

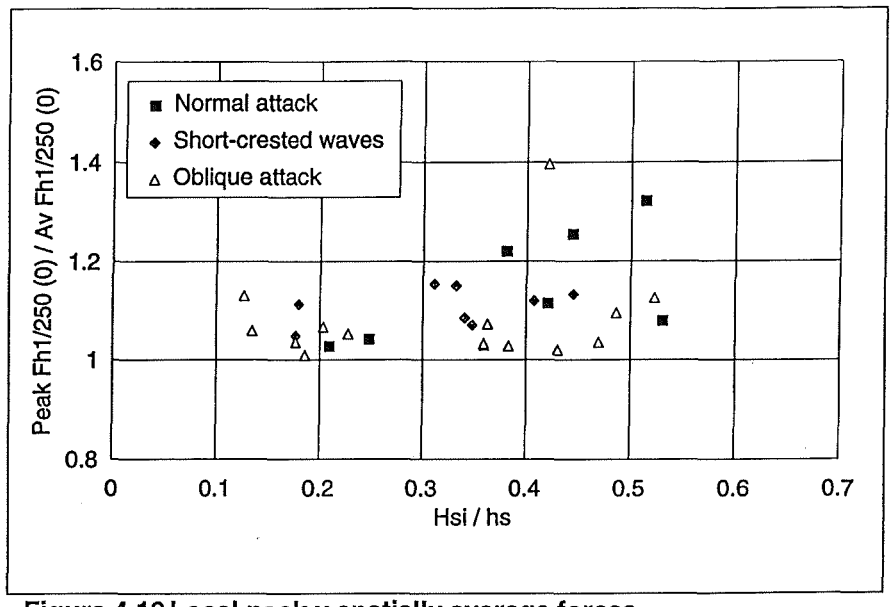

Figure 4.19 Local peak v spatially average forces

relative wave height H_{si}/h_s in Figure 4.19.

Values of $F_{h(peak)}$ / $F_{h(av)}$ reach 1.2-1.3 for normal long-crested attack. Under long-crested oblique attack, most results were much lower, not exceeding $F_{h(peak)}$ / $F_{h(av)}$ = 1.15, but with a single test giving 1.4. Under short-crested waves the ratio $F_{h(peak)}$ / $F_{h(av)}$ never exceeded 1.15, suggesting that peak forces are unlikely to exceed those analysed in this research by any substantial margin, except under conditions of normal attack. It is also reassuring to note that $F_{h(peak)}$ / $F_{h(av)}$ never exceeded 1.2 for pulsating waves, H_{si}/h_s < 0.35.

4.5 Effect of caisson length

As noted in Chapter 2, Battjes (1982) argued that oblique or short-crested wave attack on caisson of length L_c will give reductions in effective force relative to normal and/or long-crested attack, and relative to loads on a narrow strip (modelled here as a single column of transducers.

Battjes' methods give curves of a force reduction or decay coefficient, C_{Fh} in relation to caisson length, L_c/L_{op} in Figures 2.5 and 2.6 in Chapter 2. Over practical caisson lengths, those curves however show only small reductions in effective force. For most practical caissons of about 20m length, waves of T_p=7-15s with wave lengths of L_{op}=80-350m would give L_c/L_{op} from about 0.06 to 0.25. It may be noted that the longest caisson constructed to date is a single example in Japan of 100m long, giving of L_c/L_{op} = 0.3 to 1.25 for the same wave conditions.

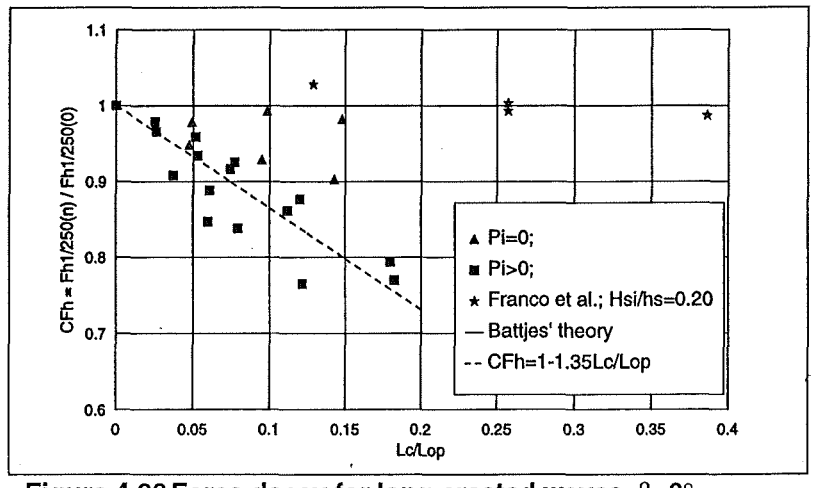

Figure 4.20 Force decay for long-crested waves, β=0°

Battjes methods were developed for simple vertical walls, so the comparisons here are based on tests with Structure 0, the simple vertical wall. The first results considered here are therefore for normal, long-crested waves in Figure 4.20. Results from these tests have been combined with results from Franco et al (1996), which show little decay over caisson lengths L_c/L_{op} up to 0.4. It has however already been noted that Franco et al's (1996) tests only measured pulsating pressures / forces.

Even for non-impact conditions, measurements of forces from this study in the CRF however show up to 10% decay, ie C_{Fh} down to 0.9 for relative caisson lengths up to L_c/L_{op}=0.15. Wave impact conditions (H_{si}/h_s>0.35), however, gave substantially greater reductions in the effective force, even over short caisson lengths, 0.005 <L_c/L_{op} <0.2.

A simple regression line has been fitted through the measurements from this study to give a reduction factor C_{Fh} in terms of relative caisson length:

$$C_{Fh} = 1 - B\,(L_c/L_{op}) \qquad (4.1)$$

Where B = 1.35 for long-crested waves and β = 0°, and the reduction is valid for $L_c/L_{op} \leq 0.2$.

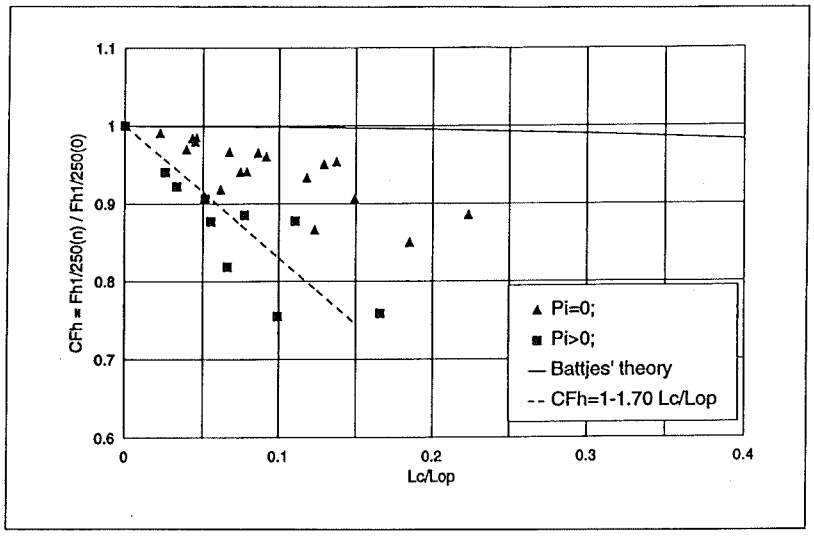

Figure 4.21 Force decay for β= 15°, long-crested waves

Under slightly oblique attack, β = 15°, forces in Figure 4.21 for non-impacting conditions show more significant reductions than for β = 0°, but there is only slightly greater change for impact conditions. The same simple form of regression line (eqn. 4.1) gives C_{Fh} in terms of L_c/L_{op}: for β = 15°, yielding B = 1.70.

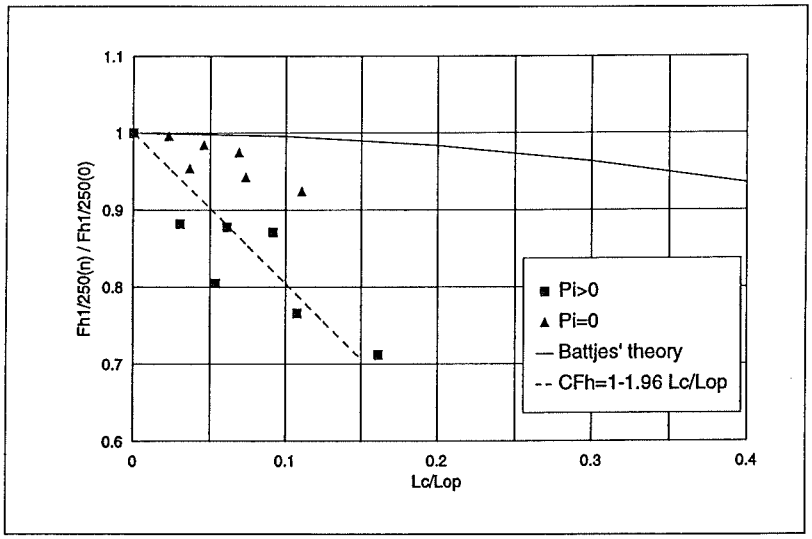

Figure 4.22 Force decay for β= 30°, long-crested waves

At greater obliquity, the force reduction is more marked for pulsating conditions, as predicted by Battjes method. Forces at β= 30° in Figure 4.22 also show slightly greater reductions for impact conditions. The same simple regression line gives B = 1.7 for β = 30°.

Short-crested waves (Figure 4.23) show no significant effect of the degree of spreading. Regression for n=2 and n=6 at β = 0° gives B = 1.56. This is steeper (greater reduction) than for long-crested waves at β = 0° (Figure 4.20), but less severe than for long-crested waves and β = 15° (Figure 4.21).

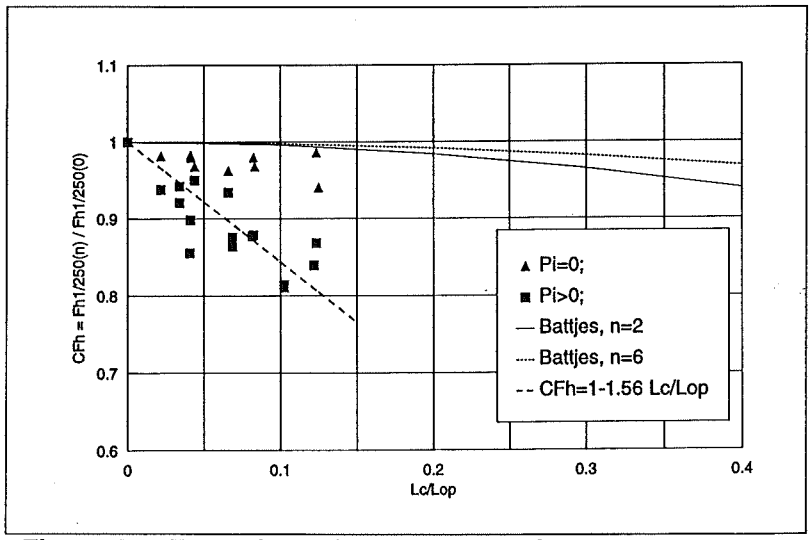

Figure 4.23 Force decay for short-crested waves

These results suggest that Battjes' model may be used to give conservative predictions under pulsating conditions, but that force reductions under impact conditions are much more significant than predicted by linear methods.

Calculations of the mean decay function on F_h (C_{Fh}) for impacting conditions can be summarised by the simple equation relating decay to relative caisson width, L_c/L_{op} in equation (4.1) where coefficient B is defined for each test case in Table 4.1 below.

Table 4.1 Impact force reduction coefficients

Wave condition	Coefficient B	Coef. Varn. (%)	Correlation r^2
Long-crested, $\beta = 0°$,	1.35	6.6	0.82
Long-crested, $\beta = 15°$,	1.69	9.2	0.77
Long-crested, $\beta = 30°$,	1.96	10.4	0.79
Short-crested, n= 2,	1.55	10.6	0.76
Short-crested, n= 6	1.58	9.3	0.77
Short-crested, n= 2, 6	1.56	6.8	0.77

5. APPLICATION OF RESULTS

The main problem of concern to this and its companion study (see SR 443) is to dimension a vertical breakwater or similar structure to resist wave action and its effects, and to deliver required hydraulic performance. The main structure design problem is therefore to dimension the caisson large enough to resist sliding or overturning forces, yet small enough to ensure optimum performance. Historically this was achieved by deriving an equivalent sliding load under pulsating wave conditions, then configuring the caisson wide and heavy enough to generate sufficient resistance to sliding. In a few instances this was extended to include overturning failure to be resisted by the bearing strength of the mound. Wave impact effects of short duration were deemed to be insignificant in relation to the inertia of a (10 – 20m long) caisson), so design methods then concentrated on the effects of longer duration wave loads caused by pulsating waves.

Early studies under the MCS-project, PROVERBS and related national research projects in UK and Germany have however demonstrated that use of pulsating loads alone may be unsafe in some circumstances as wave impacts loads have been shown to cause damage or failure. These loads become particularly important where the element concerned has relatively low inertia, and therefore has a natural period of response much closer to the (short) period of excitation of a wave impact. These types of loadings therefore become of much greater significance for wave walls, particularly when cast in short lengths; any pre-cast elements; facing panels or individual blocks.

Various prediction methods for wave forces on vertical / composite walls have been developed, but it is however not always possible to demonstrate that one particular method is more complete or more reliable than another. For such responses, it is therefore incumbent upon the user to apply alternative methods, and use engineering judgement and experience to decide which gives the most realistic result for the particular application considered.

The previous study reported by Allsop et al (1996) in report SR 443 gave a number of recommendations for analysis of wave loadings on vertical / composite walls. That report gave a new method to identify wave conditions and structure geometries where wave impact loads might be of significance. Goda's method was confirmed as giving the most realistic prediction of wave forces for pulsating waves, but new methods were suggested to predict the occurrence and estimate the magnitude of wave impact loads. The results of SR 443 were however limited to normal ($\beta = 0°$) wave attack.

This study has now examined the effects of oblique or short-crested wave attack on the occurrence and magnitude of wave impacts, and reduction factors have been developed to describe the influence on the magnitude of wave impact forces of oblique or short-crested wave conditions.

In parallel with these studies, the much larger research initiative of the PROVERBS project has led to a number of scientific advances. Some of those findings may be applied directly, but others will require further work before they can be applied directly. Within PROVERBS, a simple step-by-step analysis method was developed to form an overall structure within which each of the new / modified methods could be placed. This suggested analysis approach is summarised here for information:

Step 1: Main geometric and wave parameters

Define

Water depth and seabed gradient in front of the structure	h_s and m
Width, height and slope of front of berm in front of wall	B_b, h_b and α
Crest freeboard above water, height of caisson face	R_c and h_f
Equivalent berm width	$B_{eq} = B_b + (h_b / 2 \tan\alpha)$
Depth of water over the berm for design water level	d
Obliquity of structure to (design) wave direction	β

It should be noted that some of these parameters may take different values for different water levels, for each of which the structure may need to be analysed.

Identify design wave condition(s) given by H_{si}, T_m and T_p taking account of wave shoaling and refraction, and of depth-limited breaking. Derive peak period wave length L_{pi} in the water depth of the structure, h_s.

Use Goda's simple breaking method to calculate $H_{max} = 1.8H_s$ or $H_{max.b}$, where the breaking wave depth h_{break} is taken $5H_s$ seaward of the structure.

Step 2: First estimate of wave force / mean pressure
Use Hiroi's formula to estimate an equivalent uniform wave pressure p_{av} on the front face over a wall height h_f up to $1.25H_s$ above still water level, and hence the total horizontal force F_{Hiroi}:

$$p_{av} = 1.5\rho_w g H_s \quad (5.1a)$$
$$F_{Hiroi} = 1.5 h_f \rho_w g H_s \quad (5.1b)$$

Use F_{Hiroi} to give first estimate of breakwater width B_w to resist sliding assuming no dynamic up-lift pressures, but including buoyant up-lift, and friction $\mu = 0.5$.

Step 3: Improve calculation of horizontal and up-lift forces
Use Goda's method to predict horizontal and up-lift forces at 1/250 level, F_{hGoda} and F_{uGoda}, and related pressure distribution. Wave pressures on the front face are distributed trapezoidally, reducing from p_1 at s.w.l. to p_2 at the caisson base. Up-lift pressures are distributed triangularly from the seaward edge to zero at the rear heel.

The total horizontal force F_h (per m length of breakwater) is calculated by integrating pressures p_1, p_2 and p_3 over the front face. The total up-lift force F_u (per m of breakwater) is given by $F_u = 0.5\, p_u B_w$.

Apply Goda and/or Battjes methods to include effects of wave obliquity and/or short-crestedness on effective forces.

Using the 1/250 value, and assuming a Rayleigh distribution, pulsating wave forces at various other exceedance levels may be estimated from the following ratios of $F_{i\%}/F_{1/250}$:

Exceedance level	$F_{i\%}/F_{1/250}$
50%	0.33
90%	0.59
98%	0.77
99%	0.84
99.5%	0.90
99.8%	0.97
99.9%	1.03

Step 4: Revise estimates of caisson size
Use simple overtopping methods by Besley et al (1998) or Franco & Franco (1999) to check crest elevation against required wave transmission or overtopping limits, and confirm or revise crest freeboard, R_c.

Then use both horizontal and up-lift forces F_{hGoda}, F_{uGoda}, and revised value of R_c to revise estimate of caisson width, assuming friction $\mu = 0.6$ or other given value.

Step 5: Identify loading case using parameter map
Calculate key decision parameters:

relative berm height $h_b^* = h_b/h_s$
relative wave height $H_s^* = H_{si}/h_s$
relative berm width, $B^* = B_{eq}/L_p$.

Use these parameters in method developed in SR 443, or as revised by McConnell (1998) to determine loading case type.

Step 6: Initial calculation of impact force
If parameter map in Step 5 indicates Transition or Impact conditions, then use Allsop & Vicinanza's method to estimate an impact force, $F_{h.A\&V}$, again at 1/250 level:

$$F_{h.A\&V} = 15\, \rho_w\, g\, d^2\, (H_{si}/d)^{3.134} \quad (5.2)$$

Use this simple estimate of impact force if $F_{h.A\&V}/F_{hGoda} > 1.2$

Step 7: Estimate Pi%
Use Calabrese's method as described by Calabrese & Allsop (1998) to determine P_i. Calculate a maximum breaking wave height, $H_{99.6\%bC}$, and significant (breaking) wave height H_{sibC}, and derive estimate of $P_{i\%}$.

Note that H_{sibC} is a fictional rather than measured parameter, and may differ significantly from breaking significant wave heights determined by other methods, see particularly Weggel (1972), Owen (1980), Durand & Allsop (1997), Allsop & Durand (1998).

Use $P_{i\%}$ to decide loading case

$P_{i\%} < 2\%$	Little breaking, wave loads are primarily pulsating
$2 < P_{i\%} < 10$	Breaking waves give impacts
$P_{i\%} > 10\%$	Heavy breaking may give impacts or broken loads

Step 8: Estimate impact force using Oumeraci & Kortenhaus' method
If $P_{i\%} > 1\%$, use Oumeraci & Kortenhaus' method with coefficients as modified by McConnell & Allsop (1998) to calculate $F_{hO\&K}$.

Compare $F_{hO\&K}$ against $F_{hA\&V}$. If the difference is large, check that case is in range of the test data. Use McConnell & Allsop's comparisons of test results to decided which method gives most realistic estimate of $F_{hImpact}$.

Step 9: Estimate impact rise time
Use Oumeraci & Kortenhaus (1997) method as revised by McConnell & Allsop (1998) to estimate limiting impact rise times, t_r.

Step 10: Estimate reductions of wave impact forces with respect to wave obliquity / short-crestedness

Use method of Allsop & Calabrese (1998, 1999) to calculate impact force reduction factor, C_{Fh}:

$$C_{Fh} = 1 - B(L_c/L_{op}) \qquad (5.3)$$

Where values of B are given in Table 4.1, and the reduction is only applied to impact loads and over the range $0 < L_c/L_{op} \leq 0.2$.

Calculate the reduced impact force = $C_{Fh} \times F_{h,impact}$

Step 11: Estimate up-lift forces under impacts
If step 7 gives Impacts, use Kortenhaus & Oumeraci (1997) method to calculate up-lift force, $F_{uK\&O}$.

Step 12: Scale corrections
If condition in step 6 and/or 7 is Pulsating, scale F_{hGoda} and F_{uGoda} by Froude, ie scale correction factor of unity is applicable.

If forces are Impact in steps 6 and 7, then apply correction factor of 0.4-0.5 derived by Allsop et al (1996):

a) estimate aeration from level of $P_{i\%}$;
b) estimate attenuation of $F_{hImpact}$ from level of aeration;
c) apply scale correction to $F_{hImpact}$ based on aeration-induced attenuation.
d) scale rise time and impact duration, t_r & T_D by duration correction.

Step 13: Pressure distributions
If condition in step 6 and/or 7 is Pulsating, plot pressures calculated in step 3.

If forces are Impact in steps 6 and 7, then use new general method derived by Muller et al (1998).

6. CONCLUSIONS AND RECOMMENDATIONS

The primary objective of these experiments was to provide additional design data for vertical faced breakwaters and related structures on wave loads under oblique or short-crested wave attack. The programme of work identified at the start included:

a) Review most recent data from MAST project(s) on critical wave conditions, obliquities, and wave spreading.
b) Design and construct model caisson sections; instrument for pressures / forces.
c) Measure wave forces / pressures in parametric wave basin tests for oblique, long- and short-crested wave conditions.
d) Complete analysis to identify the influence of oblique wave attack and/or short-crested waves on wave forces. Analyse spatial variations.
e) Present study results in empirical formulae / graphs. Derive general design rules.

This series of 3-d model tests were therefore conducted to measure wave forces on vertical and composite caisson breakwaters under 3-dimensional wavve attack. The work extended the scope of the 2-d study reported by Allsop et al (1996) in SR 443 by measuring the effects of wave obliquity and wave spreading. The conclusions drawn from this study should therefore be considered in conjunction with the results of the preceding work.

The conclusions from the 3-dimensional studies may be summarised:

a) There is good agreement between results from 2-d tests in 1994 with 1:50 approach bed slope, and results from tests with normal long-crested waves in the CRF with 1:20 approach bed slope.

b) Impacts on composite walls follow the trends identified previously at Wallingford, but with some indications that impacts might start at slightly lower relative wave heights, perhaps $H_{si}/h_s \geq 0.30$. Revisions of the parameter map under PROVERBS have however indicated the onset of impacts for $H_{si}/h_s \geq 0.35$ for simple vertical walls, but for $H_{si}/d \geq 0.2$ for low mound composite walls. Results of these tests suggest that higher levels of impacts for some configurations may be reduced under 3-d conditions, even if only normal wave attack is used.

c) Under oblique long-crested waves, the occurrence of wave impacts on vertical walls are substantially reduced at β=15°, 30° and 45°. This is repeated for high mounds at β=15°, 30° and 45°, and low mounds for β=30° and 45°.

d) Effects of short-crested waves of dispersion index of 2 or more do not appear to vary significantly with increased spreading.

e) Under oblique or short-crested waves, the variation of peak forces relative to those averaged over a length equivalent to a caisson of about 20m are relatively small, not exceeding a ratio of 1.2.

f) The variation of peak force on a single narrow strip under normal wave attack is more substantial, with peak forces up to 1.3 times greater than the average.

g) Battjes' method for estimating the decay of average force with longer caissons gives very small reductions for most practical caisson lengths. The tests with pulsating conditions show that Battjes' predictions are generally conservative.

h) For impact conditions, average forces reduce significantly with caisson length, giving reductions of 25% or so over relative caisson lengths of only 0.2.

i) A simple reduction factor for F_h under impacting conditions as a function of L_c/L_{op} has been developed. Values of a coefficient B have been presented here in Table 4.1 for long-crested waves at different obliquities, and for short-crested waves.

The results of these studies also suggest the following initial conclusions on spatial correlation of impact forces under oblique / short-crested waves:

j) For heavy impacts ($F_{Impact}/F_{Goda} >> 2.5$), and small obliquity or spreading: - assume a typical coherence length $\leq L/16$;

k) For light impacts ($F_{Impact}/F_{Goda} < 2$), normal wave attack ($\beta = 0°$) and little spreading: - assume a typical coherence length $\leq L/4$;

The achievements of this work, taken together with the results from the companion study reported by Allsop et al (1996) in SR 443, may be re-stated:

- Methods to determine horizontal wave forces on vertical and composite walls have been examined, and a new method has been developed to identify geometric or wave conditions that may lead to wave impact forces. The simple parameter map developed in SR443 offers a substantial improvement over previous methods, and will identify most impact conditions of potential concern.
- The use of Goda's prediction method has been (substantially) confirmed for pulsating wave conditions.
- For those combinations of structure geometry and wave conditions at which wave impact conditions may occur, a simple method to estimate the horizontal wave impact force has been developed.
- Under oblique wave attack wave impact forces are reduced relative to the "head-on" condition. Reduction factors are suggested here for given wave obliquities.
- Short-crested waves also reduce wave impact forces, and appropriate reduction factors are also suggested.

7. ACKNOWLEDGEMENTS

The work discussed here is based on studies completed by members of the Coastal Group of HR Wallingford, the Department of Civil Engineering of the University of Sheffield, and the Department of Hydraulic and Environmental Engineering of the University of Naples. The work was conducted for the Construction Sponsorship Directorate of the UK Department of Environment, under research contract CI 39/5/96, and in part supported under the PROVERBS project of the EC's MAST III programme under contract MAS3-CT95-0041. Support for extended analysis was provided by the Ministry of Agriculture, Fisheries & Food under Flood Defence Commission FD0201.

Additional support was given by the Department of Hydraulics of University of Naples Federico II, and by the Department of Civil & Structural Engineering of University of Sheffield. Funding for visiting researchers at Wallingford was awarded by the "Programme for International Exchange of Researchers" of University of Naples Federico II, with further funding for visiting researchers at Wallingford from the TECHWARE programme of COMETT, and the National Council for Research in Italy, CNR.

The authors gratefully acknowledge assistance in testing at Wallingford by Adrian Channel, Rob Jones, Diego Vicinanza, and Alberto Bracci-Laudiero; and in processing data by Laurence Banyard, Kirsty McConnell, and Rob Jones. Early drafts of this report were assembled by Laurence Banyard with William Allsop and Mario Calabrese. Further analysis was conducted by Mario Calabrese and William Allsop.

The suggestions on spatial limitations and coherence were distilled from discussions with Professor Alberto Lamberti from Bolgna in Italy, with additional comments from Professor Hans Burcharth and Dr Peter Frigaard of Aalborg University in Denmark, which is gratefully acknowledged.

8. REFERENCES

Allsop N.W.H. (1995) "Vertical walls and breakwaters: optimization to improve vessel safety and wave disturbance by reducing wave reflections" Chapter 10 in Wave Forces on Inclined and Vertical Wall Structures, pp 232-258, ed. Kobayashi N. & Demirbilek Z., ASCE, New York.

Allsop N.W.H., Calabrese M., Vicinanza D. & Jones R.J. (1996a) "Wave impact loads on vertical and composite breakwaters" Proc. 10th Congress of the Asia and Pacific Division of IAHR, 26-29 August 1996, Langkawi Island, Malaysia

Allsop N.W.H. & Calabrese M. (1998) "Impact loadings on vertical walls in directional seas " Proceedings of 26th International Conference on Coastal engineering, June 1998, Copenhagen, publn. ASCE, New York.

Allsop N.W.H. & Durand N. (1998) "Influence of steep seabed slopes on breaking waves for structure design " Proceedings of 26th International Conference on Coastal Engineering, June 1998, Copenhagen, publn. ASCE, New York.

Allsop NWH, Vicinanza D, & McKenna JE (1996b) "Wave forces on vertical and composite breakwaters" Strategic Research Report SR 443, HR Wallingford, March 1996, Wallingford.

Allsop N.W.H. & Vicinanza D. (1996) "Wave impact loadings on vertical breakwaters: development of new prediction formulae " Proc. 11th Int. Harbour Congress, pp 275-284, Royal Flemish Society of Engineers, Antwerp, Belgium.

Battjes J (1982). "Effects of short-crestedness on wave loads on long structures" Journal of Applied Ocean Research, Vol 4 No 3 pp 165-172.

Besley P.B., Stewart T, & Allsop N.W.H. (1998) "Overtopping of vertical structures: new methods to account for shallow water conditions" Proceedings of Int. Conf. on Coastlines, Structures & Breakwaters '98, March 1998, Institution of Civil Engineers / Thomas Telford, London, pp46-57.

British Standards Institution (1984) "British Standard Code of practice for Maritime structures, Part 1. General Criteria" BS 6349: Part 1: 1984, and Amendments 5488 and 5942, British Standards Institution, London.

British Standards Institution (1991) "British Standard Code of practice for Maritime structures, Part 7. Guide to the design and construction of breakwaters" BS 6349: Part 7: 1991, British Standards Institution, London.

Calabrese M. (1997) "Onset of breaking in front of vertical and composite breakwaters " Paper 1.0.4 to PROVERBS Task 1 workshop, Edinburgh, July 1997, pp 13 publn. HR Wallingford.

Calabrese M. & Allsop N.W.H. (1997) "Impact loadings on vertical walls in directional seas" Paper 1.2.7 to PROVERBS Task 1 workshop, Edinburgh, July 1997, pp 16 publn. HR Wallingford.

Calabrese M., Vicinanza D. & Allsop N.W.H. (1996) "Azioni idrodinamiche su dighe marittime a parete verticale - Influenza della geometria dell'imbasamento", XXV Convegno di Idraulica e Costruzioni Idrauliche, Torino, Settembre 1996.

CERC (1984) "Shore Protection Manual" 4th ed. U.S. Govt. Printing Office, Washington D.C.

Centurioni L., Vicinanza D. & Allsop N.W.H. (1995) "Wave forces on vertical walls: analysis methods for measurements of pressures and forces" Report IT 430, HR Wallingford.

Durand N. & Allsop N.W.H. (1998) "Effects of steep bed slopes on depth-limited wave breaking" Proceedings of Waves '97 Conference, November 1997, Virginia Beach, publn. ASCE, New York.

Franco L., Franco C., Passoni G, Restano, & Van der Meer JW. (1995) Paper 4.8 in the final report of the MCS - project, Publn University of Hannover.

Franco C., Meer J.W. van der, & Franco L (1996) "Multi-directional wave loads on vertical breakwaters" Proc 25th Int. Conf. on Coastal Eng., Orlando, publn. ASCE, New York.

Franco C. & Franco L. (1999) "Overtopping formulae for caisson breakwaters with non-breaking 3-d waves" Jo. Waterway, Port, Coastal & Ocean Engineering, Vol 125, No 2, March / April 1999, ASCE, New York, pp 98-107.

Goda Y. (1974) "New wave pressure formulae for composite breakwaters" Proc. 14th ICCE, Copenhagen, ASCE, New York.

Goda Y. (1985) "Random seas and maritime structures" University of Tokyo Press, Tokyo.

Goda Y. (1994) "Dynamic response of upright breakwaters to impulsive breaking wave forces" Coastal Engineering, Special Issue on Vertical Breakwaters, Vol 22, pp 135-158, Elsevier Science BV, Amsterdam.

Goda Y. (1995) "Japan's design practice in assessing wave forces on vertical breakwaters" Chapter 6 in Wave Forces on Inclined and Vertical wall Structures, pp140-155, ed. Kobayashi N. & Demirbilek Z., ASCE, New York.

Hunt J. N. (1979). "Direct solution of wave dispersion equation" Journal of Waterways and Harbours Division, Proc ASCE, vol WW4, November 1979, pp457-459, ASCE, New York.

Lamberti A. & Franco L. (1994) "Italian experience on upright breakwaters" Proceedings of Workshop on Wave Barriers in Deep Waters, pp25-75, Port and Harbour Research Institute, Yokosuka, Japan.

Madurini L. & Allsop N.W.H. (1995) "Overtopping performance of vertical and composite breakwaters and seawalls: results of wave flume tests" Paper II.4.2 to the Final MCS Project Workshop, Alderney, publn University of Hannover.

McBride M.W., Allsop N.W.H., Besley P., Colombo D. & Madurini L. (1995) "Vertical walls and low reflection alternatives: results of wave flume tests on reflections and overtopping" Report IT 417, HR Wallingford, Wallingford.

McBride M.W., Smallman J.V. & Allsop N.W.H. (1996) "Guidelines for the hydraulic design of harbour entrances" Report SR 430, HR Wallingford, Wallingford.

McBride M.W., & Watson G.M. (1995) "Vertical walls and low reflection alternatives: results of 3-d physical model tests" Report IT 425, HR Wallingford, Wallingford.

McKenna J.E (1997) "Wave forces on caissons and breakwater crown walls" PhD thesis, Department of Civil & Struct. Eng., Queen's University of Belfast, Belfast.

Oumeraci H. (1994) "Review and analysis of vertical breakwater failures - lessons learned" Coastal Engineering, Special Issue on Vertical Breakwaters Vol. 22, pp. 3-29, Elsevier Science BV, Amsterdam.

Oumeraci H. (1995) "European multi-disciplinary research experience on vertical breakwaters: the MCS project" Proceedings Second MAST Days and EUROMAR market, 7-10 November 1995, pp 737-762, publn. Directorate General of Science, Research and Development, European Commission, Brussels.

Oumeraci H. & Kortenhaus K. (1997) Wave impact loading – tentative formulae and suggestions for the development of final formulae. Proceedings 2nd PROVERBS Task 1 Workshop, Edinburgh, publn. HR Wallingford.

Owen M W (1980) "Design of sea walls allowing for wave overtopping" Report EX 924, Hydraulics Research, Wallingford.

Tanimoto K. & Takahashi S. (1994) "Design and construction of caisson breakwaters - the Japanese experience" Coastal Engineering, Vol 22, pp57-78, Elsevier Science BV, Amsterdam.

Thomas RS & Hall B (1991) "Sea wall design guidelines" CIRIA / Butterworths, London.

Weggel J.R. (1972) "Maximum breaker height" Jo. Waterway, Harbour and Coastal Eng. Div., Proc. ASCE, Vol. 98, No WW4, pp 529-548, publn. ASCE, New York.

Appendices

Appendix 1

Table of test conditions

Appendix 1 Table of test conditions

Structure	Wave conditions H_s (m)	T_m (s)	Long-crested or Short-crested Spreading, n	SWL (m)	s_m	Dir	N	T_{mo} (s)	T_{mi} (s)	H_{so} (m)	H_{si} (m)	$H_{i\,99.6}$ (m)	H_{si}/d	d (m)	B_b (m)
Structure 0															
10000	0.10	1.80	l-c	0.77	0.02	45	500	1.86	1.74	0.126	0.070	0.087	0.135	0.52	
10001	0.10	1.30	l-c	0.77	0.04	45	500	1.38	1.28	0.125	0.066	0.092	0.127	0.52	
10002	0.10	1.80	l-c	0.77	0.02	30	500	1.85	1.92	0.101	0.106	0.13	0.203	0.52	
10003	0.20	2.50	l-c	0.77	0.02	30	500	2.34	2.25	0.231	0.187		0.360	0.52	
10004	0.20	1.50	l-c	0.77	0.06	30	500	1.53	1.58	0.205	0.189	0.274	0.363	0.52	
10005	0.25	2.00	l-c	0.77	0.04	30	500	2.03	2.03	0.254	0.253	0.302	0.487	0.52	
10006	0.10	1.80	l-c	0.77	0.02	15	500	1.71	1.73	0.094	0.097	0.126	0.186	0.52	
10007	0.10	1.30	l-c	0.77	0.04	15	500	1.3	1.32	0.091	0.092		0.177	0.52	
10008	0.20	2.50	l-c	0.77	0.02	15	500	2.37	2.28	0.199	0.224	0.305	0.431	0.52	
10009	0.20	1.80	l-c	0.77	0.04	15	500	1.79	1.76	0.190	0.199	0.261	0.383	0.52	
10010	0.20	1.50	l-c	0.77	0.06	15	500	1.43	1.41	0.194	0.187	0.259	0.360	0.52	
10011	0.25	2.00	l-c	0.77	0.04	15	500	1.95	1.97	0.231	0.272	0.368	0.523	0.52	
10012	0.10	1.80	l-c	0.77	0.02	0	500	1.6	1.65	0.104	0.109		0.210	0.52	
10013	0.20	2.50	l-c	0.77	0.02	0	500	2.21	2.18	0.215	0.219	0.326	0.421	0.52	
10014	0.20	1.50	l-c	0.77	0.06	0	200	1.45	1.51	0.194	0.198	0.289	0.381	0.52	
10015	0.25	2.00	l-c	0.77	0.04	0	500	1.84	1.87	0.262	0.276		0.531	0.52	
10016	0.10	1.80	s-c, n=2	0.77	0.02	0	500	1.74	1.77	0.089	0.092		0.177	0.52	
10017	0.20	2.50	s-c, n=2	0.77	0.02	0	500	2.4	2.48	0.150	0.162		0.312	0.52	
10018	0.20	1.80	s-c, n=2	0.77	0.04	0	500	1.75	1.78	0.172	0.173		0.333	0.52	
10019	0.25	2.00	s-c, n=2	0.77	0.04	0	500	1.92	1.94	0.208	0.212		0.408	0.52	
10020	0.10	1.80	s-c, n=6	0.77	0.02	0	500	1.75	1.77	0.093	0.094		0.180	0.52	
10021	0.20	2.50	s-c, n=6	0.77	0.02	0	500	2.4	2.48	0.168	0.181		0.348	0.52	
10022	0.20	1.80	s-c, n=6	0.77	0.04	0	500	1.76	1.77	0.179	0.177		0.341	0.52	
10023	0.25	2.00	s-c, n=6	0.77	0.04	0	500	1.92	1.94	0.232	0.232		0.445	0.52	
10024	0.10	1.80	l-c	0.68	0.02	0	500	1.63	1.68	0.101	0.107	0.158	0.249	0.43	
10025	0.20	2.50	l-c	0.68	0.02	0	500	2.18	2.18	0.211	0.221	0.33	0.514	0.43	
10026	0.20	1.50	l-c	0.68	0.06	0	500	1.44	1.51	0.189	0.191	0.271	0.444	0.43	
10027	0.10	1.80	l-c	0.68	0.02	15	500	1.66	1.76	0.093	0.098	0.149	0.228	0.43	
10028	0.20	2.50	l-c	0.68	0.02	15	500	2.21	2.44	0.212	0.202	0.331	0.470	0.43	

Structure	Wave conditions H_s (m)	T_m (s)	Long-crested or Short-crested Spreading, n	SWL (m)	s_m	Dir	N	T_{mo} (s)	T_{mi} (s)	H_{so} (m)	H_{si} (m)	$H_{i\ 99.6}$ (m)	H_{si}/d	d (m)	B_b (m)
10029	0.20	1.50	l-c	0.68	0.06	15	500	1.51	1.47	0.185	0.181	0.249	0.421	0.43	
10030	0.10	1.80	l-c	0.77	0.02	15	2000	1.71	1.73	0.094	0.097	0.126	0.186	0.52	
10031	0.10	1.30	l-c	0.77	0.04	15	2000	1.3	1.32	0.091	0.092		0.177	0.52	
10032	0.20	2.50	l-c	0.77	0.02	15	2000	2.37	2.28	0.199	0.224	0.305	0.431	0.52	
10033	0.20	1.80	l-c	0.77	0.04	15	2000	1.79	1.76	0.190	0.199	0.261	0.383	0.52	
10034	0.20	1.50	l-c	0.77	0.06	15	2000	1.43	1.41	0.194	0.187	0.259	0.360	0.52	
10035	0.25	2.00	l-c	0.77	0.04	15	2000	1.95	1.97	0.231	0.272	0.368	0.523	0.52	
Reversed directions														0.52	
10036	0.10	1.80	l-c	0.77	0.02	15	500	1.71	1.73	0.094	0.097	0.126	0.186	0.52	
10037	0.10	1.80	l-c	0.77	0.02	15	500	1.71	1.73	0.094	0.097	0.126	0.186	0.52	
10038	0.20	2.50	l-c	0.77	0.02	15	500	2.37	2.28	0.199	0.224	0.305	0.431	0.52	
10039	0.20	2.50	l-c	0.77	0.02	15	500	2.37	2.28	0.199	0.224	0.305	0.431	0.52	
10040	0.20	1.80	l-c	0.77	0.04	15	500	1.79	1.76	0.190	0.199	0.261	0.383	0.52	
10041	0.20	1.80	l-c	0.77	0.04	15	500	1.79	1.76	0.190	0.199	0.261	0.383	0.52	
10042	0.25	2.00	l-c	0.77	0.04	15	500	1.95	1.97	0.231	0.272	0.368	0.523	0.52	
10043	0.25	2.00	l-c	0.77	0.04	15	500	1.95	1.97	0.231	0.272	0.368	0.523	0.52	
10000Hz tests														0.43	
10070	0.10	1.80	l-c	0.68	0.02	15	500	1.66	1.76	0.093	0.098	0.149	0.228	0.43	
10071	0.20	2.50	l-c	0.68	0.02	15	500	2.21	2.44	0.212	0.202	0.331	0.470	0.43	
10072	0.20	1.50	l-c	0.68	0.06	15	500	1.51	1.47	0.185	0.181	0.249	0.421	0.43	
Structure 1															
1000	0.10	1.80	l-c	0.77	0.02	45	500	1.86	1.74	0.126	0.070	0.087	0.210	0.333	0.25
1001	0.10	1.30	l-c	0.77	0.04	45	500	1.38	1.28	0.125	0.066	0.092	0.199	0.333	0.25
1002	0.10	1.80	l-c	0.77	0.02	30	500	1.85	1.92	0.101	0.106	0.13	0.318	0.333	0.25
1003	0.20	2.50	l-c	0.77	0.02	30	500	2.34	2.25	0.231	0.187		0.562	0.333	0.25
1004	0.20	1.50	l-c	0.77	0.06	30	500	1.53	1.58	0.205	0.189	0.274	0.568	0.333	0.25
1005	0.25	2.00	l-c	0.77	0.04	30	500	2.03	2.03	0.254	0.253	0.302	0.760	0.333	0.25
1006	0.10	1.80	l-c	0.77	0.02	15	500	1.71	1.73	0.094	0.097	0.126	0.291	0.333	0.25
1007	0.10	1.30	l-c	0.77	0.04	15	500	1.3	1.32	0.091	0.092		0.276	0.333	0.25

Structure	Wave conditions H_s (m)	T_m (s)	Long-crested or Short-crested Spreading, n	SWL (m)	s_m	Dir	N	T_{mo} (s)	T_{mi} (s)	H_{so} (m)	H_{si} (m)	$H_{i\ 99.6}$ (m)	H_{si}/d	d (m)	B_b (m)
1008	0.20	2.50	l-c	0.77	0.02	15	500	2.37	2.28	0.199	0.224	0.305	0.673	0.333	0.25
1009	0.20	1.80	l-c	0.77	0.04	15	500	1.79	1.76	0.190	0.199	0.261	0.598	0.333	0.25
1010	0.20	1.50	l-c	0.77	0.06	15	500	1.43	1.41	0.194	0.187	0.259	0.562	0.333	0.25
1011	0.25	2.00	l-c	0.77	0.04	15	500	1.95	1.97	0.231	0.272	0.368	0.817	0.333	0.25
1012	0.10	1.80	l-c	0.77	0.02	0	500	1.6	1.65	0.104	0.109		0.327	0.333	0.25
1013	0.20	2.50	l-c	0.77	0.02	0	500	2.21	2.18	0.215	0.219	0.326	0.658	0.333	0.25
1014	0.20	1.50	l-c	0.77	0.06	0	500	1.45	1.51	0.194	0.198	0.289	0.595	0.333	0.25
1015	0.25	2.00	l-c	0.77	0.04	0	500	1.84	1.87	0.262	0.276		0.829	0.333	0.25
1016	0.10	1.80	s-c, n=2	0.77	0.02	0	500	1.74	1.77	0.089	0.092		0.276	0.333	0.25
1017	0.20	2.50	s-c, n=2	0.77	0.02	0	500	2.4	2.48	0.150	0.162		0.486	0.333	0.25
1018	0.20	1.80	s-c, n=2	0.77	0.04	0	500	1.75	1.78	0.172	0.173		0.520	0.333	0.25
1019	0.25	2.00	s-c, n=2	0.77	0.04	0	500	1.92	1.94	0.208	0.212		0.637	0.333	0.25
1020	0.10	1.80	s-c, n=6	0.77	0.02	0	500	1.75	1.77	0.093	0.094		0.281	0.333	0.25
1021	0.20	2.50	s-c, n=6	0.77	0.02	0	500	2.4	2.48	0.168	0.181		0.544	0.333	0.25
1022	0.20	1.80	s-c, n=6	0.77	0.04	0	500	1.76	1.77	0.179	0.177		0.532	0.333	0.25
1023	0.25	2.00	s-c, n=6	0.77	0.04	0	500	1.92	1.94	0.232	0.232		0.695	0.333	0.25
1024	0.10	1.80	l-c	0.68	0.02	0	500	1.63	1.68	0.101	0.107	0.158	0.440	0.243	0.25
1025	0.20	2.50	l-c	0.68	0.02	0	50	2.18	2.18	0.211	0.221	0.33	0.909	0.243	0.25
1026	0.20	1.50	l-c	0.68	0.06	0	500	1.44	1.51	0.189	0.191	0.271	0.786	0.243	0.25
1027	0.10	1.80	l-c	0.68	0.02	15	500	1.66	1.76	0.093	0.098	0.149	0.403	0.243	0.25
1028	0.20	2.50	l-c	0.68	0.02	15	500	2.21	2.44	0.212	0.202	0.331	0.831	0.243	0.25
1029	0.20	1.50	l-c	0.68	0.06	15	500	1.51	1.47	0.185	0.181	0.249	0.745	0.243	0.25
Structure 2															
2000	0.10	1.80	l-c	0.77	0.02	45	500	1.86	1.74	0.126	0.070	0.087	0.300	0.233	0.25
2001	0.10	1.30	l-c	0.77	0.04	45	500	1.38	1.28	0.125	0.066	0.092	0.284	0.233	0.25
2002	0.10	1.80	l-c	0.77	0.02	30	500	1.85	1.92	0.101	0.106	0.13	0.454	0.233	0.25
2003	0.20	2.50	l-c	0.77	0.02	30	500	2.34	2.25	0.231	0.187		0.803	0.233	0.25
2004	0.20	1.50	l-c	0.77	0.06	30	500	1.53	1.58	0.205	0.189	0.274	0.811	0.233	0.25
2005	0.25	2.00	l-c	0.77	0.04	30	500	2.03	2.03	0.254	0.253	0.302	1.086	0.233	0.25

Structure	Wave conditions H_s (m)	T_m (s)	Long-crested or Short-crested Spreading, n	SWL (m)	s_m	Dir	N	T_{mo} (s)	T_{mi} (s)	H_{so} (m)	H_{si} (m)	$H_{i\ 99.6}$ (m)	H_{si}/d	d (m)	B_b (m)
2006	0.10	1.80	l-c	0.77	0.02	15	500	1.71	1.73	0.094	0.097	0.126	0.415	0.233	0.25
2007	0.10	1.30	l-c	0.77	0.04	15	500	1.3	1.32	0.091	0.092		0.395	0.233	0.25
2008	0.20	2.50	l-c	0.77	0.02	15	500	2.37	2.28	0.199	0.224	0.305	0.961	0.233	0.25
2009	0.20	1.80	l-c	0.77	0.04	15	500	1.79	1.76	0.190	0.199	0.261	0.855	0.233	0.25
2010	0.20	1.50	l-c	0.77	0.06	15	500	1.43	1.41	0.194	0.187	0.259	0.803	0.233	0.25
2011	0.25	2.00	l-c	0.77	0.04	15	500	1.95	1.97	0.231	0.272	0.368	1.167	0.233	0.25
2012	0.10	1.80	l-c	0.77	0.02	0	500	1.6	1.65	0.104	0.109		0.850	0.233	0.25
2013	0.20	2.50	l-c	0.77	0.02	0	500	2.21	2.18	0.215	0.219	0.326	0.940	0.233	0.25
2014	0.20	1.50	l-c	0.77	0.06	0	200	1.45	1.51	0.194	0.198	0.289	0.850	0.233	0.25
2015	0.25	2.00	l-c	0.77	0.04	0	500	1.84	1.87	0.262	0.276		1.185	0.233	0.25
2016	0.10	1.80	s-c, n=2	0.77	0.02	0	500	1.74	1.77	0.089	0.092		0.395	0.233	0.25
2017	0.20	2.50	s-c, n=2	0.77	0.02	0	500	2.4	2.48	0.150	0.162		0.695	0.233	0.25
2018	0.20	1.80	s-c, n=2	0.77	0.04	0	500	1.75	1.78	0.172	0.173		0.742	0.233	0.25
2019	0.25	2.00	s-c, n=2	0.77	0.04	0	500	1.92	1.94	0.208	0.212		0.910	0.233	0.25
2020	0.10	1.80	s-c, n=6	0.77	0.02	0	200	1.75	1.77	0.093	0.094		0.402	0.233	0.25
2021	0.20	2.50	s-c, n=6	0.77	0.02	0	500	2.4	2.48	0.168	0.181		0.777	0.233	0.25
2022	0.20	1.80	s-c, n=6	0.77	0.04	0	500	1.76	1.77	0.179	0.177		0.761	0.233	0.25
2023	0.25	2.00	s-c, n=6	0.77	0.04	0	500	1.92	1.94	0.232	0.232		0.994	0.233	0.25
2024	0.10	1.80	l-c	0.68	0.02	0	500	1.63	1.68	0.101	0.107	0.158	0.748	0.143	0.25
2025	0.20	2.50	l-c	0.68	0.02	0	500	2.18	2.18	0.211	0.221	0.33	1.545	0.143	0.25
2026	0.20	1.50	l-c	0.68	0.06	0	500	1.44	1.51	0.189	0.191	0.271	1.336	0.143	0.25
2027	0.10	1.80	l-c	0.68	0.02	15	500	1.66	1.76	0.093	0.098	0.149	0.685	0.143	0.25
2028	0.20	2.50	l-c	0.68	0.02	15	500	2.21	2.44	0.212	0.202	0.331	1.413	0.143	0.25
2029	0.20	1.50	l-c	0.68	0.06	15	500	1.51	1.47	0.185	0.181	0.249	1.266	0.143	0.25
Structure 3															
3000	0.10	1.80	l-c	0.77	0.02	15	500	1.71	1.73	0.094	0.097	0.126	0.529	0.183	0.25
3001	0.10	1.30	l-c	0.77	0.04	15	500	1.3	1.32	0.091	0.092		0.503	0.183	0.25
3002	0.20	2.50	l-c	0.77	0.02	15	500	2.37	2.28	0.199	0.224	0.305	1.224	0.183	0.25
3003	0.20	1.80	l-c	0.77	0.04	15	500	1.79	1.76	0.190	0.199	0.261	1.089	0.183	0.25
3004	0.20	1.50	l-c	0.77	0.06	15	500	1.43	1.41	0.194	0.187	0.259	1.022	0.183	0.25
3005	0.25	2.00	l-c	0.77	0.04	15	500	1.95	1.97	0.231	0.272	0.368	1.486	0.183	0.25

Structure	Wave conditions H_s (m)	T_m (s)	Long-crested or Short-crested Spreading, n	SWL (m)	s_m	Dir	N	T_{mo} (s)	T_{mi} (s)	H_{so} (m)	H_{si} (m)	$H_{i\ 99.6}$ (m)	H_{si}/d	d (m)	B_b (m)
3006	0.10	1.80	l-c	0.77	0.02	0	500	1.6	1.65	0.104	0.109		1.082	0.183	0.25
3007	0.20	2.50	l-c	0.77	0.02	0	500	2.21	2.18	0.215	0.219	0.326	1.197	0.183	0.25
3008	0.20	1.50	l-c	0.77	0.06	0	500	1.45	1.51	0.194	0.198	0.289	1.082	0.183	0.25
3009	0.25	2.00	l-c	0.77	0.04	0	500	1.84	1.87	0.262	0.276		1.508	0.183	0.25
3010	0.10	1.80	l-c	0.68	0.02	0	500	1.63	1.68	0.101	0.107	0.158	1.151	0.093	0.25
3011	0.20	2.50	l-c	0.68	0.02	0	500	2.18	2.18	0.211	0.221	0.33	2.376	0.093	0.25
3012	0.20	1.50	l-c	0.68	0.06	0	500	1.44	1.51	0.189	0.191	0.271	2.054	0.093	0.25
3013	0.10	1.80	l-c	0.68	0.02	15	500	1.66	1.76	0.093	0.098	0.149	1.054	0.093	0.25
3014	0.20	2.50	l-c	0.68	0.02	15	500	2.21	2.44	0.212	0.202	0.331	2.172	0.093	0.25
3015	0.20	1.50	l-c	0.68	0.06	15	500	1.51	1.47	0.185	0.181	0.249	1.946	0.093	0.25
Mono frequency tests															
Structure 0	(H)	(T)													
10044	0.20	2.07		0.77		0	10						0.385	0.52	
10045	0.30	2.87		0.77		0	10						0.577	0.52	
10046	0.30	1.72		0.77		0	10						0.577	0.52	
10047	0.10	2.07		0.77		0	10						0.192	0.52	
10048	0.10	1.50		0.77		0	10						0.192	0.52	
10049	0.20	2.07		0.77		15	10						0.385	0.52	
10050	0.20	1.50		0.77		15	10						0.385	0.52	
10051	0.30	2.87		0.77		15	10						0.577	0.52	
10052	0.30	2.07		0.77		15	10						0.577	0.52	
10053	0.30	1.72		0.77		15	10						0.577	0.52	
10054	0.10	2.07		0.77		15	10						0.192	0.52	
10055	0.10	1.50		0.77		15	10						0.192	0.52	
10056	0.10	1.15		0.77		15	10						0.192	0.52	
10057	0.20	2.07		0.77		30	10						0.385	0.52	
10058	0.30	2.87		0.77		30	10						0.577	0.52	
10059	0.30	1.72		0.77		30	10						0.577	0.52	
10060	0.10	2.07		0.77		30	10						0.192	0.52	

Structure	Wave conditions H_s (m)	T_m (s)	Long-crested or Short-crested Spreading, n	SWL (m)	s_m	Dir	N	T_{mo} (s)	T_{mi} (s)	H_{so} (m)	H_{si} (m)	$H_{i\ 99.6}$ (m)	H_{si}/d	d (m)	B_b (m)
10061	0.10	1.50		0.77		30	10						0.192	0.52	
10062	0.20	2.07		0.68		0	10						0.465	0.43	
10063	0.30	2.87		0.68		0	10						0.698	0.43	
10064	0.30	1.72		0.68		0	10						0.698	0.43	
10065	0.10	2.07		0.68		0	10						0.233	0.43	
10066	0.20	2.07		0.68		15	10						0.465	0.43	
10067	0.30	2.87		0.68		15	10						0.698	0.43	
10068	0.30	1.72		0.68		15	10						0.698	0.43	
10069	0.10	2.07		0.68		15	10						0.233	0.43	

Appendix 2

Modification of pressure analysis program for 3-d tests

Appendix 2 Modification of pressure analysis program for 3-d tests – K J McConnell

This appendix details modifications to a pressure analysis program, which was originally written to analyse data from 2-d tests. The modifications were required to allow analysis of data from the 3-d tests. This appendix is intended to complement the information in Centurioni et al (1995), which described the original program. The modified program is called "prescal3".

A2.1 Summary of modifications

The original program was specific to the structural configurations tested and the facility in which the 2-d study was carried out. It was necessary to extract from the program information specific to the 2-d tests and replace this with variables read from a number of control files.

The original program analysed 16 transducers in a specific configuration with transducers situated on the face and base of the caisson and in the mound. The program was modified to deal with up to 20 transducers in a series of columns on the face of the caisson.

As up-lift pressures were not measured in the 3-d tests, the calculation of maximum forces was simplified. In the original program, horizontal and up-lift forces were calculated with their corresponding moments. The modified version was only required to calculate horizontal forces on the front face, but needed to give information on lateral variations. Horizontal forces were calculated firstly for each column of transducers in turn and then for various combinations of columns, thus allowing quantification of the variation of the horizontal force with caisson length.

The modifications result in a program which can be used for analysis of a variety of configurations of pressure transducers, with the exception of the calculation of forces. This is carried out in one subroutine, written specifically for the analysis required. Use of the program for other configurations would require that only this subroutine be changed.

A2.2 Description of program

The program starts by reading in the data from the control file "inp.dat", an example of which is given in Table A2.1. This contains parameters such as the test name, the number of transducers, the frequency of acquisition, details of the filenames, the transducer to be used for definition of the pressure events (normally at Still Water Level), the mean period and the still water level. The hydrostatic pressure is then calculated at each of the transducers. This is followed by the event definition which ensures that only the largest pressure peak is logged in those events where multiple peaks occur. Once all the events have been defined, the record for each transducer in turn is analysed to find the peak pressure for each event. For each peak, the pressures at the other transducers at the same time are written to the same file. Force intensities are averaged over various combinations of caisson length with the maxima for each event being recorded. Finally, the pressure rise time, Δ t, from the start of the event to the peak, is calculated for each event.

Table A2.1 Input file - inp.dat

```
        test -  test name  (prescal3)
'c31568c'
        itrans - no of transducers (max 20)
18
        ifreq - rate of acquisition of data(Hz)
400
        namefilei -  SWL file name
o.dac
        namefiles - first file to analyze
a.dac
        namefilee - last file to analyze
r.dac
        period - average period (s)
1.5
        swl - SWL (m above datum)
0.68
end
```

A2.3 Modifications

A2.3.1 Naming of output files

The names of the output files were modified. A list and explanation of the output obtained is given below :

file	output
stats.out	data derived from pressure record for calculation of initial noise level
noisef.out	noise level
	frequency of occurrence of noise level reading
pres.out	hydrostatic pressure at each transducer
events.out	start time of event
info.out	date
	time
	test number
	mean period
	Still Water Level
	Number of points
	static water level
	sampling frequency
	number of events
	pressure at static water level
	elapsed time

The following information is obtained per transducer:

file	output
peaks.*	start time of event
	end time of event
	maximum pressure (kN/m^2) at transducer * for that event
	time of maximum pressure
	minimum pressure (kN/m^2) at transducer * for that event
	time of minimum pressure
	pressures at all transducers (18) at that time (in kN/m^2)
deltat.*	pressure rise time
	time of initiation of pressure increase for each event

where * is the letter of the transducer, in this case, from 'a' to 'r'.

The following information is output for the forces, for various combinations of caissons, ie various caisson lengths:

file	output
max*.fh	maximum value of force intensity (kN/m) in an event for the combination *
	time of maximum force
	pressures at all transducers (18) at that time (in kN/m^2)

where * indicates the combination of columns which the file gives data for (see Section A2.3.5).

A2.3.2 Inp.dat

This input file has been modified to include more parameters which had previously been implicit in the program. The number of transducers was read in from "inp.dat" The original program was written specifically for the analysis of 16 transducers. The rate of acquisition of pressures is read in from "inp.dat". This was previously included in the program as a value of 400Hz.

A2.3.3 Calculation of hydrostatic pressure

Hydrostatic pressure at the start of the tests is calculated in the subroutine "statpres". This reads in the initial voltage recorded at the transducer from the file "medaver.dat". This is then multiplied by the calibration factor a and added to the offset b, which are read from the file "calfac.dat". Examples of "medaver.dat" and "calfac.dat" are given in Tables A2.2 and A2.3 respectively.

Table A2.2 Input file - medaver.dat

1.557373E-01
7.272949E-02
7.080078E-04
-1.806641E-03
1.911621E-02
2.197266E-04
4.131348E-01
3.443115E-01
2.588135E-01
9.289551E-02
9.504394E-02
1.298096E-01
1.579102E-01
7.106934E-02
-1.376953E-02
-2.441406E-05
-1.914063E-02
-2.155762E-02

Table A2.3 Input file - calfac.dat

1.006881	-0.09019
1.010198	-0.11796
1.006712	-0.04002
1.010372	-0.04201
1.012419	-0.12141
1.00203	-0.13199
1.023754	-0.19589
0.99204	-0.09278
1.005614	0.030595
1.022838	-0.00276
1.013152	-0.07119
1.055656	-0.04042
1.016669	-0.08233
1.013625	-0.10349
1.008516	-0.06021
1.006658	-0.07678
1.002639	-0.12438
1.001948	-0.12085

The modified version differs from the original program which calculated the hydrostatic pressure in one of three ways: either statistically from the beginning of the transducer record, theoretically from the Still Water Level and the positions of the transducers or by inputting the known values of hydrostatic pressure at each transducer.

A2.3.4 Event definition

Two criteria must be satisfied to define the start of an event. Firstly the pressure must be above a predetermined threshold. This is a function of the noise level and is derived as described in Centurioni et al (1995). Secondly, the pressure must show a sustained increase over a given length of time. This is done by ensuring that the ratio of the two running averages, "sumfor" and "sumback" is greater than 1.1 for a duration of $T_m/10$. These two running averages are summed over 20 pressure records, with "sumback" being 1 timestep behind "sumfor". In the original analysis program a duration of $T_m/6$ was used to define the start of the event, but this missed some smaller events in the 3-d testing as smaller wave heights have been used, resulting in smaller pressures being recorded.

A2.3.5 Calculation of forces

The calculation of force intensity is done in subroutine "forces". This subroutine was written to meet specifically the requirements of the 3-d analysis. In the tests there were 3 vertical columns of 6 transducers. The average force intensity (kN/m length) is calculated for each of these columns. Force intensity for other lengths of caisson are calculated by averaging the force intensity over various combinations of columns. The configuration of the transducers is shown in **Figure 3.4**. The combinations for which force intensity was calculated are as follows:

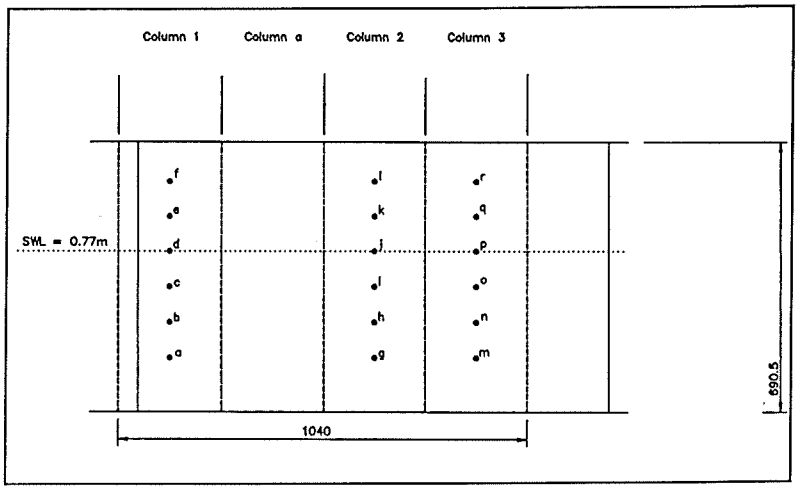

column 1
column 2
column 3
columns 2 and 3
columns 1, a and 2
columns a, 2 and 3
columns 1, a, 2 and 3

This covered 3 caisson lengths of 0.26m (2 column), 0.52m (3 columns) and 0.78m (4 columns) and also considered a strip of infinitely short length (1 column).

For combinations which included column a, the pressures acting here were taken as an average of those acting on columns 1 and 2.

The forces on any one column are calculated using the staircase method. This involves multiplying the pressure at a transducer by the area it represents, doing this for all the transducers considered and dividing the result by the length covered, in order to obtain a force intensity in kN/m. The areas which each transducer represented were included in the original program. The program was modified to read these in from the file "facelocn.dat". An example of the file "facelocn.dat" is given in Table A2.4. This file contains a second column of numbers which are the area multiplied by a lever arm, for the calculation of moments. Moments were not calculated for the analysis completed for this study, but the input file was given this format to maintain the option of the calculation of moments for future use of the program.

Table A2.4 Input file - facelocn.dat

0.04758	0.006566
0.0234	0.005335
0.0234	0.007441
0.0234	0.009547
0.0234	0.011653
0.03835	0.02255
0.04758	0.006566
0.0234	0.005335
0.0234	0.007441
0.0234	0.009547
0.0234	0.011653
0.03835	0.02255
0.04758	0.006566
0.0234	0.005335
0.0234	0.007441
0.0234	0.009547
0.0234	0.011653
0.03835	0.02255

The maximum force intensity per event was written to a file with the pressures at each of the 18 transducers. One file was created for each combination of columns.

A2.4 Problems during data acquisition

Structure 2

During data acquisition in the CRF, transducer b failed to record data for the tests on the second composite structure, structure 2. A modified version of the program was used to analyse the C2 tests, replacing the data for transducer b with an average of transducers a and c. This version of the program is called "prescal4".

Wave condition C1

During acquisition for the tests with wave condition C1, transducer g at the bottom of the second column did not record data properly. This was modified by using the data at transducer h for both locations.

References

Centurioni L., Vicinanza D. & Allsop N.W.H. (1995) "Wave forces on vertical walls: analysis methods for measurements of pressures and forces" Report IT 430, HR Wallingford.